Acta Pharmaceutica Sinica B 2025;15(3):1397−1414

Chinese Pharmaceutical Association
Institute of Materia Medica, Chinese Academy of Medical Sciences

Acta Pharmaceutica Sinica B

www.elsevier.com/locate/apsb
www.sciencedirect.com

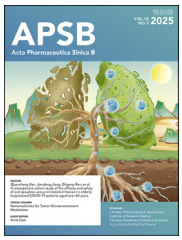

ORIGINAL ARTICLE

Nitazoxanide protects against heart failure with preserved ejection and metabolic syndrome induced by high-fat diet (HFD) plus L-NAME "two-hit" in mice

Jiahui Chen, Liping Zhang, Ting Xie, Xiao Zhang, Congcong Pan, Fangli Sun, Wenfeng Li, Zhijie Sun*, Deli Dong*

Department of Pharmacology, China Pharmaceutical University, Nanjing 211198, China

Received 3 August 2024; received in revised form 10 December 2024; accepted 17 December 2024

KEY WORDS

Nitazoxanide;
Tizoxanide;
HFpEF;
Metabolic syndrome;
Heart hypertrophy;
Heart fibrosis;
Hepatic steatosis

Abstract The clinical antiprotozoal drug nitazoxanide has been demonstrated to improve the experimental diabetes mellitus, lipid metabolism disorders, atherosclerosis and inhibit inflammation. Since the pathogenesis of heart failure with preserved ejection (HFpEF) is multifactorial and closely associated with the aforementioned diseases, we aim to study the effect of nitazoxanide on high-fat diet (HFD) plus L-NAME (*Nω*-nitro-L-arginine methyl ester)-induced HFpEF and metabolic syndrome in mice. We found that oral nitazoxanide improved cardiac hypertrophy, cardiac fibrosis, cardiac diastolic dysfunction, increased blood pressure, impaired exercise tolerance, impaired glucose handling, serum lipid disorders, hepatic steatosis, increased weight of white adipose tissues and kidney fibrosis in HFD + L-NAME-treated mice. In the established HFD + L-NAME-induced HFpEF and metabolic syndrome mouse model, therapeutic treatment with nitazoxanide rescued HFD + L-NAME-induced pathological phenotypes as mentioned above. The *in vitro* experiments revealed that tizoxanide, the active metabolite of nitazoxanide, increased the basal mitochondria metabolism of cardiomyocytes, inhibited cardiomyocyte hypertrophy and collagen secretion from cardiac fibroblasts, and relaxed phenylephrine- and U46619-induced constriction of rat mesenteric arteries, indicating that the direct effect of tizoxanide might partly contribute to the protective effect of nitazoxanide against HFpEF *in vivo*. The present study suggests that nitazoxanide might be a potential drug for HFpEF and metabolic syndrome therapy.

*Corresponding authors.
E-mail addresses: dongdeli@cpu.edu.cn (Deli Dong), sunzhijie@cpu.edu.cn (Zhijie Sun).

Peer review under the responsibility of Chinese Pharmaceutical Association and Institute of Materia Medica, Chinese Academy of Medical Sciences.

https://doi.org/10.1016/j.apsb.2024.12.040

1. Introduction

Heart failure with preserved ejection fraction (HFpEF) is associated with hypertension, diabetes, lipid metabolic disorders, obesity, aging, etc. Epidemiological studies have shown that more than 50% of heart failure patients are HFpEF patients. Presently, only sacubitril-valsartan and sodium-glucose co-transporter 2 inhibitors dapagliflozin and empagliflozin are approved for HFpEF therapy. A recent randomized controlled trial demonstrated that semaglutide, a glucagon-like peptide 1 receptor agonist, reduced heart failure-related symptoms and physical limitations among patients with obesity-related HFpEF and type 2 diabetes mellitus[1], indicating that glucagon-like peptide 1 receptor agonists are new candidates for HFpEF therapy.

The pathogenesis of HFpEF is complex and associated with cardiac hypertrophy, cardiac fibrosis, vascular endothelial injury, abnormal glucose and lipid metabolism, inflammation, aging, etc. The multifactorial mechanisms of HFpEF pathogenesis indicate that the ideal anti-HFpEF drugs should have the effects of improving metabolic abnormalities, inflammation, cardiac hypertrophy, cardiac fibrosis and vascular dysfunction simultaneously.

Our previous studies about mitochondrial uncouplers have provided inspiration for finding novel anti-HFpEF drugs. We found that the mitochondrial uncouplers with different chemical structure exhibited common pharmacological effects, including cardiomyocyte protection[2], AMPK activation and vasodilation[3-6], and inhibition of NLRP3 inflammasome activation[7,8]. Nitazoxanide is an FDA-approved drug for diarrhea caused by *Cryptosporidium* and *Giardia intestinalis*. Nitazoxanide has a good safety profile. A dose of 1000 mg/day of nitazoxanide in clinical trials for 48 weeks showed no significant adverse effects[9,10]. We found that nitazoxanide and its active metabolite tizoxanide were mitochondrial uncouplers. Nitazoxanide and tizoxanide activated cellular AMPK, inhibited NF-κB signaling and NLRP3 inflammasome activation[8,11]. The clinical equivalent doses of nitazoxanide improved experimental hyperlipidemia and hepatic steatosis in hamsters and mice and inhibited atherosclerosis in mice[8,11]. Our latest work demonstrated that both nitazoxanide and tizoxanide exerted an anti-aging effect on *Caenorhabditis elegans*[12]. Based on the multiple effects of nitazoxanide and tizoxanide mentioned above, we hypothesize that nitazoxanide might be protective against HFpEF and metabolic syndrome.

2. Materials and methods

2.1. Animals

The HFpEF mouse model was established by using the high-fat diet (HFD) + *N*ω-nitro-L-arginine methyl ester (L-NAME) "two-hit" method with a slight modification[13]. The specific pathogen-free male C57BL/6N mice (20−25 g, 8 weeks old) were obtained from Gempharmatech Co., Ltd. (Nanjing, China). All animals were kept at 24 °C with a 12-h light, 12-h dark cycle and unlimited to access water and food. For the preventive experiments, following a week of acclimatization, the mice were randomly assigned to ND (normal diet) (n = 18), HFD + L-NAME (n = 18), HFD + L-NAME + Nitazoxanide (100, 150, 200/75 mg/kg, #01088480, Adamas-beta, Shanghai, China) (n = 18) and HFD + L-NAME + Dapagliflozin (2 mg/kg, AstraZeneca Pharmaceuticals LP, Delaware, DE, USA) (n = 18) groups based on the body weight. For HFD + L-NAME + Nitazoxanide (200/75 mg/kg) group, the mice received 200 mg/kg for the first 8 weeks, followed by 75 mg/kg for the remaining 12 weeks.

In the therapeutic experiments, the mice were initially divided into ND and HFD + L-NAME groups and were treated with ND and HFD + L-NAME respectively for 7 weeks to establish the HFpEF model. After confirming the model establishment, HFD + L-NAME-treated mice were randomly divided into HFD + L-NAME group (n = 15), HFD + L-NAME + Nitazoxanide (150 mg/kg) group (n = 15) and HFD + L-NAME + Dapagliflozin (2 mg/kg) (n = 15) group, and were treated for additional 9 weeks.

All the mice in different groups were treated with drugs once daily. The mice in ND and HFD + L-NAME groups were gavaged with an appropriate volume of solvent (0.5% methylcellulose) and the mice in HFD + L-NAME + Nitazoxanide and HFD + L-NAME + Dapagliflozin groups were gavaged with the corresponding doses of drugs. The mice were euthanized following anesthesia with 2,2,2-tribromoethanol (2.5%, 0.12 mL/10 g, i.p., #T48402, Sigma, St. Louis, MO, USA) at the termination of the experiment. The ND (fat content 10%, #M10110C2) and HFD (fat content 60%, #M23010401) were purchased from Biopike Co., Ltd. (Shanghai, China). L-NAME (#51298-62-5, YuanyeBio-Technology Co., Ltd., Shanghai, China) was embedded into the high-fat diet (1 g/kg). Experimentation was approved by the Committee for Animal Research of China Pharmaceutical University (Approval No. 2023-03-025) and adhered to the Guide for the Care and Use of Laboratory Animals.

2.2. Echocardiography analysis

Transthoracic echocardiography was performed by using the VisualSonics Vevo 3100LT system equipped with an MX400 transducer. Anesthesia was induced by 1%−3% isoflurane (#R510-22-10, RWD, Shenzhen, China) and confirmed by the lack of response to firm pressure on the tails. The heart rate of mice was maintained at 400−500 beats/min. EF%, FS%, LVAW (d), LVAW (s), LVPW (d), LVPW (s), LVID (d), LVID (s), LV mass, cardiac output, volume (d), volume (s), diameter (d), diameter (s) and stroke volume were measured in the parasternal long axis section under M-mode condition. E and A waves were measured in the flow spectrum of the mitral valve under the Pulse-wave mode at the maximum mitral valve opening on the four-chamber incisal plane. At the end of the procedures, all mice recovered from anesthesia. All parameters were measured at least three times, and the means were used.

2.3. Oral glucose tolerance test

The oral glucose tolerance test (OGTT) was conducted by gavage of glucose (2 g/kg in saline) following a 6-h fast. The tail blood glucose

levels (mmol/L) were assessed by using a glucometer (Accu-Chek Active, Roche Diagnostics, Mannheim, Germany) before (0 min) and 30, 60, 90 and 120 min after glucose administration.

2.4. Tail-cuff blood pressure recording

The tail cuff method was used to measure the tail artery blood pressure of conscious mice by using an animal non-invasive blood pressure monitor (Kent Scientific, Shanghai, China). The mice were placed in a restrainer on a temperature-regulated platform (37 °C) and the blood pressure was measured under calm, stable conditions. All mice had undergone acclimation training prior to the formal measurements.

2.5. Exercise exhaustion test

After three days of adaptive training to treadmill exercise (NJKEWBIO, Nanjing, China), an exhaustion test was conducted following this procedure: starting at an initial velocity of 10 m/min for 180 s, then increasing the velocity to 18 m/min. The exhaustion was defined as: when the mice reached the electric-stimulus grid which had 0.5 mA stimulating current, they were unable to run again within 10 s. The running distance was recorded to assess exercise tolerance.

2.6. Grip-strength test

The sarcous strength was assessed by using the grip-strength test (Xinruan Information Technology Co., Ltd., Shanghai, China). The limbs or forelimbs of mice gripped the net or "T" pole which connected with the sensor. The operator gently pulled the mice's tail horizontally until the limbs or forelimbs were released. The peak force (g) was measured and recorded three times to evaluate sarcous strength.

2.7. Histology

Hematoxylin−eosin (H&E, #G1120, Solarbio, Beijing, China) staining was used to observe the morphological characteristics of the liver and kidney or to calculate the cross-sectional area of adipose cells. Masson's trichrome staining (#G1346, Solarbio) was used to evaluate the fibrosis area in the heart and kidney. Oil red O (#A600395, Sangon Biotech, Shanghai, China) staining was used to evaluate the degree of lipid deposition in the liver and kidney. Wheat germ agglutinin (WGA, #W11262, Thermo Fisher Scientific, Waltham, MA, USA) staining was used to determine the cross-sectional area of cardiomyocytes. All tissues were fixed in 4% paraformaldehyde or embedded with O.C.T. Compound (#4583, Sakura Finetek USA Inc., Torrance, CA, USA), sectioned at 5 or 10 μm, and then processed according to the kit instructions. Images were captured by using a microscope (Olympus, Tokyo, Japan) with 20 × and 40 × objectives.

2.8. Serum experiments

The level of serum N-terminal proBNP (NT-proBNP) was detected by enzyme-linked immunosorbent assays in accordance with the manufacturer's protocols (#E-EL-M0834c, Elabscience, Wuhan, China). The levels of serum total cholesterol (TC, #A111-1-1), triglycerides (TG, #A110-1-1), high-density lipoprotein cholesterol (HDL-C, #A112-1-1), low-density lipoprotein cholesterol (LDL-C, #A113-1-1), aspartate aminotransferase (AST, #C010-2-1) and alanine transaminase (ALT, #C009-2-1) were detected by enzymatic colorimetric methods in accordance with the manufacturer's protocols (Jiancheng, Nanjing, China).

2.9. Hepatic lipid analysis

The hepatic and cardiac lipid levels were measured by using commercial kits according to the manufacturer's protocols (#E1025 and #E1026, Applygen, Beijing, China). Briefly, the tissues were lysed and homogenized at 4 °C. A portion of the homogenate was centrifuged at 2000 × *g* (D1524R, DLAB Scientific Co., Ltd., Beijing, China) for 5 min after incubation at 70 °C for 10 min. The supernatants were used to determine the concentrations of TG and TC. The remaining homogenate was used to measure the protein concentration of tissues by using the BCA Protein Assay Kit (#P0012, BeyoTime, Shanghai, China).

2.10. Western blot

The total protein extraction and separation were conducted according to our previous works[8,14,15]. Equal amounts of protein were separated by electrophoresis on 10%−12.5% SDS-PAGE gels and then transferred to nitrocellulose membranes. After blocked with 5% skim milk for 1 h, the membranes were incubated with specific antibodies at 4 °C overnight. After washing with TBS-0.1% Tween 20, the membranes were then exposed to fluorescence-labeled goat anti-mouse IgG (1:10,000, #926e32210, LI-COR Biosciences, Lincoln, NE, USA) or goat anti-rabbit IgG (1:10,000, #926e32211, LI-COR Biosciences) at room temperature for 1 h. Signals were visualized by using the Odyssey Dlx Infrared Imaging System (LI-CO Biosciences). Protein levels were quantified by using Image Studio 5.0 software (LI-CO Biosciences). The antibodies used for Western blot were as following: β-actin (1:8000, #bs-0061R, Bioss, Beijing, China), ANP (1:1000, #A14755, Abclonal, Wuhan, China), BNP (1:1000, #A23996, Abclonal), Col-1 (1:1000, #14695-1-AP, Proteintech), β-MHC (1:3000, #M8421, Sigma, St. Louis, MO, USA), p-AMPKα (Thr172) (1:1000, #2535, Cell Signaling Technology, Danvers, MA, USA), AMPKα (1:1000, #2532, Cell Signaling Technology), p-Akt (Ser473) (1:1000, #4060, Cell Signaling Technology), Akt (1:1000, #9272, Cell Signaling Technology), p-STAT3 (Y705) (1:1000, #9145, Cell Signaling Technology), STAT3 (1:1000, #4904, Cell Signaling Technology).

2.11. Isolation and culture of neonatal mice cardiomyocytes and cardiac fibroblasts

The hearts of ICR mice (Jiangsu Huachuang Sino Pharma Tech Co., Ltd., Nanjing, China) for 1−2 days were removed and washed with cold PBS 3 times, followed by washing with Hank's Balanced Salt Solution (HBSS, #BL559A, Biosharp, Hefei, China). The hearts were incubated with 6 mL HBSS and 3 mL trypsin (#T1300, Solarbio) at 4 °C overnight. Subsequently, the hearts were digested with Collagenase Type II (0.8 mg/mL, #9001-12-1, Gibco). The cells were then suspended in Dulbecco's modified Eagle's medium/medium (DMEM, #C11995500, Gibco) supplemented with 15% fetal bovine serum (FBS, #TN-10099141, Gibco), 100 U/mL penicillin and 100 μg/mL streptomycin (#C0222, Beyotime, Shanghai, China). The cell suspension was evenly distributed into multiple culture flasks and placed in a humidified incubator (95% air−5% CO_2) for 60 min to allow for the selective adhesion of cardiac fibroblasts. Subsequently, the suspended cardiomyocytes were transferred to a separate culture

flask. The purity of the cultured primary cardiomyocytes and cardiac fibroblasts was assessed by using immunofluorescence staining, respectively, as shown in Supporting Information Fig. S1. The purity of the cultured primary cardiomyocytes reached 95%, while the cardiac fibroblasts reached about 99%.

After being stimulated with phenylephrine (PE, 100 μmol/L, #07220202, Harvest Pharmaceutical Co., Ltd., Shanghai, China), TGF-β1 (10 ng/mL, #MA0626, Meilunbio, Dalian, China) or IL-6 (50 ng/mL, #216-16, Proteintech, Wuhan, China) and treated with different concentrations of tizoxanide (1, 2, 5, 10 μmol/L, #HY-12687, MCE, USA) for 24 h, the cells were used for immunofluorescence and Western blot analysis.

2.12. Immunofluorescence staining

The cardiomyocytes and cardiac fibroblasts were washed with cold phosphate-buffered solution (PBS) three times for 10 min and fixed with 4% paraformaldehyde at room temperature for 10 min. After washing with cold PBS, the cells were permeabilized with 0.2% Triton X-100 for 1 h and blocked with goat serum for 1 h. Vimentin antibody (#19607, Abclonal) and α-actinin (#69758S, Cell Signaling Technology) were used to incubate the cells overnight at 4 °C. The next day, the cells were washed in PBS and incubated with secondary antibodies (#ab150079 and #150113, Abcam, Cambridge, UK) for 30 min, then PBS was used to wash 3 times for 5 min. DAPI (#C0060, Solarbio) was used to stain the nucleus for 8 min. Fluorescence images were obtained by the fluorescence microscope (Olympus, Tokyo, Japan).

The area of primary cardiomyocytes was accessed by fluorescent phalloidine staining. In short, the primary cardiomyocytes were fixed with cold 4% paraformaldehyde and permeabilized with 0.5% Triton X-100. Subsequently, the primary cardiomyocytes were incubated with phalloidine at room temperature for 20 min, then PBS was used to wash 3 times for 5 min. DAPI was used to stain the nucleus for 8 min. Fluorescence images were obtained by the fluorescence microscope (Olympus, Tokyo, Japan).

2.13. Mesenteric artery tension measurement

Adult male Sprague−Dawley rats (250−300 g, purchased from Changsheng Biotechnology, Shenyang, China) were euthanized following anesthesia with 2,2,2-tribromoethanol (2.5%, 1 mL/100 g, i.p.). The mesenteric arteries were excised and placed in a cold physiological saline solution (PSS). Subsequently, the arteries were trimmed into 2-mm rings after the removal of adipose tissues. As per experiment requirements, the endothelium was denuded by cannulating the lumen and gently rubbing.

The methodologies for measuring mesenteric artery function adhered to our previous works[3,4,16]. The mesenteric artery rings were secured in a bath containing 5 mL of PSS continuously aerated with a gas mixture of 95% O_2 and 5% CO_2. The isometric constrictions of arterial rings were monitored by utilizing a multiwire myograph system (model 620 DMT, Danish MyoTechnology, Denmark). Acetylcholine (ACh, #A6625, Sigma) served as a pharmacological agent to assess endothelial integrity. In arteries with intact endothelium, Ach (1 μmol/L) induced relaxation of phenylephrine (PE, 5 μmol/L)-precontracted arteries, but Ach did not induce relaxation of arteries with denuded endothelium. PE (5 μmol/L) and U46619 (1 μmol/L, #56985-40-1, Cayman Chemical, Ann Arbor, MI, USA) were used as the vasoconstriction stimuli.

2.14. Thoracic aorta tension measurement

The mice were euthanized following anesthesia with 2,2,2-tribromoethanol. The thoracic aorta was excised and sectioned into 2-mm rings after fat tissue removal. Subsequently, the arterial rings were placed in a chamber containing 5 mL PSS, which was continuously aerated with a gas mixture (95% O_2 + 5% CO_2). The isometric constrictions of arterial rings were recorded by using a multiwire myograph system (model 620 DMT, Danish MyoTechnology, Denmark). PE and high K^+ PSS (60 mmol/L K^+) were used to induce vasoconstriction. Ach at concentrations ranging from 10^{-9} to 10^{-5} mol/L was utilized to assess endothelium-dependent vasodilation of the aorta pre-contracted by PE (10 μmol/L). The KPSS (60 mmol/L K^+) was composed of (mmol/L): NaCl, 74.7; KCl, 60; $MgSO_4 \cdot 7H_2O$, 1.17; KH_2PO_4, 1.18; $NaHCO_3$, 14.9; $CaCl_2$, 1.6; D-glucose, 5.5; EDTA, 0.026.

2.15. Mitochondrial respiratory function measurement

The mitochondrial respiratory function of cardiomyocytes and heart tissues was measured by using high-resolution respirometry (Oxygraph-2k, Oroboros Instruments, Innsbruck, Austria) as described in our previous works[17,18].

The cardiomyocytes were harvested through trypsin digestion and centrifuged at 100 × *g* (DM0412, DLAB Scientific Co., Ltd., Beijing, China) for 5 min at room temperature, and resuspended in cell culture medium without serum. The final density of the cell suspension was approximately 1 × 10^6 cells/mL. After the cell resuspension solution was stabilized in the measuring chamber for 5 min, the concentration of O_2 was adjusted. Routine respiration was followed by oligomycin (Omy, 5 nmol/L, #O4876, Sigma, St. Louis, MO, USA) titration to induce the non-phosphorylating leak state. Once the respiration stabilized, tizoxanide and the same volume of DMSO were added. Respectively, the final concentrations of tizoxanide were 0.5, 1, 2, 5, 10 μmol/L in each step. Rotenone (Rot, 0.5 μmol/L, #R8875, Sigma) and antimycin A (Ama, 2.5 μmol/L, #A8674, Sigma) were then added to assess the residual respiration. ATP production was detected by sequential titration of Omy (0.5 nmol/L), FCCP (0.5 μmol/L, #A8674, Sigma) and Ama (2.5 μmol/L) after tizoxanide (5 μmol/L) and the same volume of DMSO were added. The difference of OCR value before and after Omy treatment represented the mitochondrial ATP production[15,19].

The heart tissue (3−4 mg) was homogenized in the mitochondrial respiratory medium and the homogenate was added to calibrated chambers to evaluate the effect of tizoxanide on the activities of mitochondrial complex I, complex II, and complex IV. After the homogenate was equilibrated in the chamber for 5 min, tizoxanide (5 μmol/L) and the same volume of DMSO were added. Pyruvic acid (P, 5 mmol/L, #P2256, Sigma), *g*lutamic acid (G, 10 mmol/L, #G1626, Sigma) and malic acid (M, 2 mmol/L, #M1000, Sigma) were used to provide substrates for complex I. Rotenone (0.5 μmol/L) was used to inhibit the function of complex I, and then the substrate of complex II succinate acid (S, 10 mmol/L, #S2378, Sigma) was added. Ama (2.5 μmol/L) was used to inhibit the function of complex III. Ascorbate acid (As, 2 mmol/L, #A7631, Sigma) and *N*, *N*, *N*′, *N*′-tetramethyl-*p*-phenylenediamine dihydrochloride (Tm, 0.5 mmol/L, #T3134, Sigma) were provided as substrates for complex IV.

MiR05 consisted of: EGTA (0.5 mmol/L, #E4378, Sigma), $MgCl_2 \cdot 6H_2O$ (3 mmol/L, #MA0036, Scharlau, Barcelona, Spain), lactobionic acid (60 mmol/L, #L109639, Aladdin, Shanghai,

China), taurine (20 mmol/L, #T0625, Sigma), KH_2PO_4 (10 mmol/L, #104873, Merck, Darmstadt, Germany), HEPES (20 mmol/L, #1112GR100, Biofroxx, Einhausen, Germany), D-sucrose (110 mmol/L, #S391, PhytoTech Labs, Lenexa, KS, USA), BSA, essentially fatty acid-free (1 g/L, #BS260, Biosharp, Hefei, China).

2.16. Statistical analysis

Data are presented as mean ± standard error of mean (SEM). All figures were produced by using GraphPad Prism Version 8.0 (GraphPad Software Inc., San Diego, CA, USA) and data were analyzed by using SPSS 22.0 software (version 22.0, SPSS Inc., Chicago, IL, USA). Statistical significance was evaluated by using Student's *t*-test for comparison of two groups or one-way ANOVA for multiple comparison followed by Tukey's *post hoc* test. For data with the control value of 1 and no SEM, the Mann−Whitney *U* test was used[20]. $P < 0.05$ was considered significant.

3. Results

3.1. Oral nitazoxanide improves the HFpEF phenotypes induced by HFD + L-NAME in mice

HFD + L-NAME (endothelial nitric oxide synthase inhibitor) "two-hit"-induced mouse HFpEF mimics the clinical HFpEF phenotypes[21]. Accordingly, we established the HFD + L-NAME-induced HFpEF mouse model. Male C57BL/6N mice were divided into six groups (details were described in the Method section): ND group, HFD + L-NAME group, HFD + L-NAME + nitazoxanide (Nit) (100 mg/kg), HFD + L-NAME + Nit (150 mg/kg), HFD + L-NAME + Nit (200/75 mg/kg, 200 mg/kg was administered for the first 8 weeks, then 75 mg/kg for the remaining 12 weeks) and HFD + L-NAME + Dapagliflozin (Dapa) (2 mg/kg) group (Fig. 1A). The aim of designing the HFD + L-NAME + Nit (200/75 mg/kg) group was to evaluate the effect of the regimen with an initial high dose of nitazoxanide to achieve optimal therapy followed by a lower dose for maintenance. Dapagliflozin (2 mg/kg) was a positive drug, which was therapeutic for HFpEF in clinic[22,23].

The body weight of the mice at the end of the experiment showed that the body weight of mice in HFD + L-NAME group was higher than in the ND group. However, the body weight of mice in all HFD + L-NAME + Nit groups was lower than that in HFD + L-NAME group, and there was no significant difference of the mouse body weight between HFD + L-NAME and HFD + L-NAME + Dapa groups (Fig. 1B). The representative heart images of different groups were displayed in Fig. 1C. Since the body weight of mice in HFD + L-NAME and HFD + L-NAME + Dapa groups was higher than that in ND and HFD + L-NAME + Nit groups (Fig. 1B), in addition to the heart weight data (Fig. 1D), the ratio of heart weight to tibial length was further analyzed (Fig. 1E). The results showed that both nitazoxanide and dapagliflozin treatments prevented HFD + L-NAME-induced increase of heart weight in mice. Next, WGA staining was used to assess cardiomyocyte size in heart tissues. As shown in Fig. 1F and G, there was a significant increase of cardiomyocyte size in mice from HFD + L-NAME group compared to ND group, and the increase was mitigated by nitazoxanide and dapagliflozin treatments. Masson's trichrome staining results illustrated that HFD + L-NAME treatment also led to cardiac fibrosis, which was ameliorated by nitazoxanide and dapagliflozin treatments (Fig. 1H and I). The inhibitory effect of nitazoxanide and dapagliflozin on cardiac hypertrophy and cardiac fibrosis induced by HFD + L-NAME treatment in mice were further validated by the assessment of cardiac hypertrophy markers ANP, BNP, β-MHC and cardiac fibrosis marker collagen-1 protein levels in the heart tissues (Fig. 1J and K).

HFD + L-NAME "two-hit" induces heart diastolic dysfunction, which is the key pathological characterization of HFpEF[21]. We used the echocardiography technique to evaluate the cardiac function of mice. As shown in Fig. 1L and M, the parameter E/A ratio reflecting the heart diastolic function increased in HFD + L-NAME-treated mice and the increase was inhibited by nitazoxanide and dapagliflozin treatments; however, there was no difference of both EF(%) and FS(%) among the groups. These results suggested that nitazoxanide treatment improved HFD + L-NAME-induced heart diastolic dysfunction in mice. Additional echocardiographic parameters are shown in Supporting Information Fig. S2.

The level of plasma NT-proBNP rises in heart failure patients and NT-proBNP serves as a diagnostic biomarker for heart failure[24]. We measured the serum NT-proBNP level of mice. As shown in Fig. 1N, serum NT-proBNP level increased in HFD + L-NAME-treated mice, and the increases were inhibited by nitazoxanide and dapagliflozin treatments.

3.2. Oral nitazoxanide inhibits the increased blood pressure, restores the impaired exercise tolerance and grip force induced by HFD + L-NAME treatment in mice

HFD + L-NAME "two-hit" increases blood pressure in mice[21]. We measured the systolic blood pressure (SBP), diastolic blood pressure (DBP) and mean blood pressure (MBP) of mice at the 7th and 16th week after treatment, respectively. As shown in Fig. 2A and B, compared to ND group, the SBP, DBP and MBP of mice in HFD + L-NAME group significantly increased at the 7th and 16th week, and these increases were inhibited by both nitazoxanide and dapagliflozin treatments.

HFD + L-NAME "two-hit" reduces exercise tolerance in mice[21]. At the 17th week post-treatment, the exercise tolerance of mice was evaluated by measuring the running distance through an exercise exhaustion test. Compared to ND group, the exercise tolerance of mice in HFD + L-NAME group decreased, but the impaired exercise tolerance was improved by nitazoxanide treatment (100, 150 mg/kg) (Fig. 2C). We further measured the grip force of mice at the end of the 18th week. As shown in Fig. 2D, nitazoxanide and dapagliflozin treatments restored the decreased forelimb- and four-limb force induced by HFD + L-NAME in mice.

3.3. Nitazoxanide improves the impaired glucose handling and serum lipid disorders in HFD + L-NAME-treated mice

HFD + L-NAME "two-hit" induces glucose intolerance in mice[21]. At the end of 15th week post-treatment, we performed an OGTT. HFD + L-NAME treatment elevated fasting glucose levels (Fig. 3A) and resulted in higher glucose levels during OGTT in mice (Fig. 3B). Nitazoxanide and dapagliflozin treatments significantly improved HFD + L-NAME-induced glucose handling impairment in mice (Fig. 3A−C).

At the experiment termination, we measured the serum lipids including TG, TC, LDL-C and HDL-C. HFD + L-NAME treatment induced significant increases of serum TC, LDL-C and HDL-C levels (Fig. 3D−G). Nitazoxanide treatment reduced

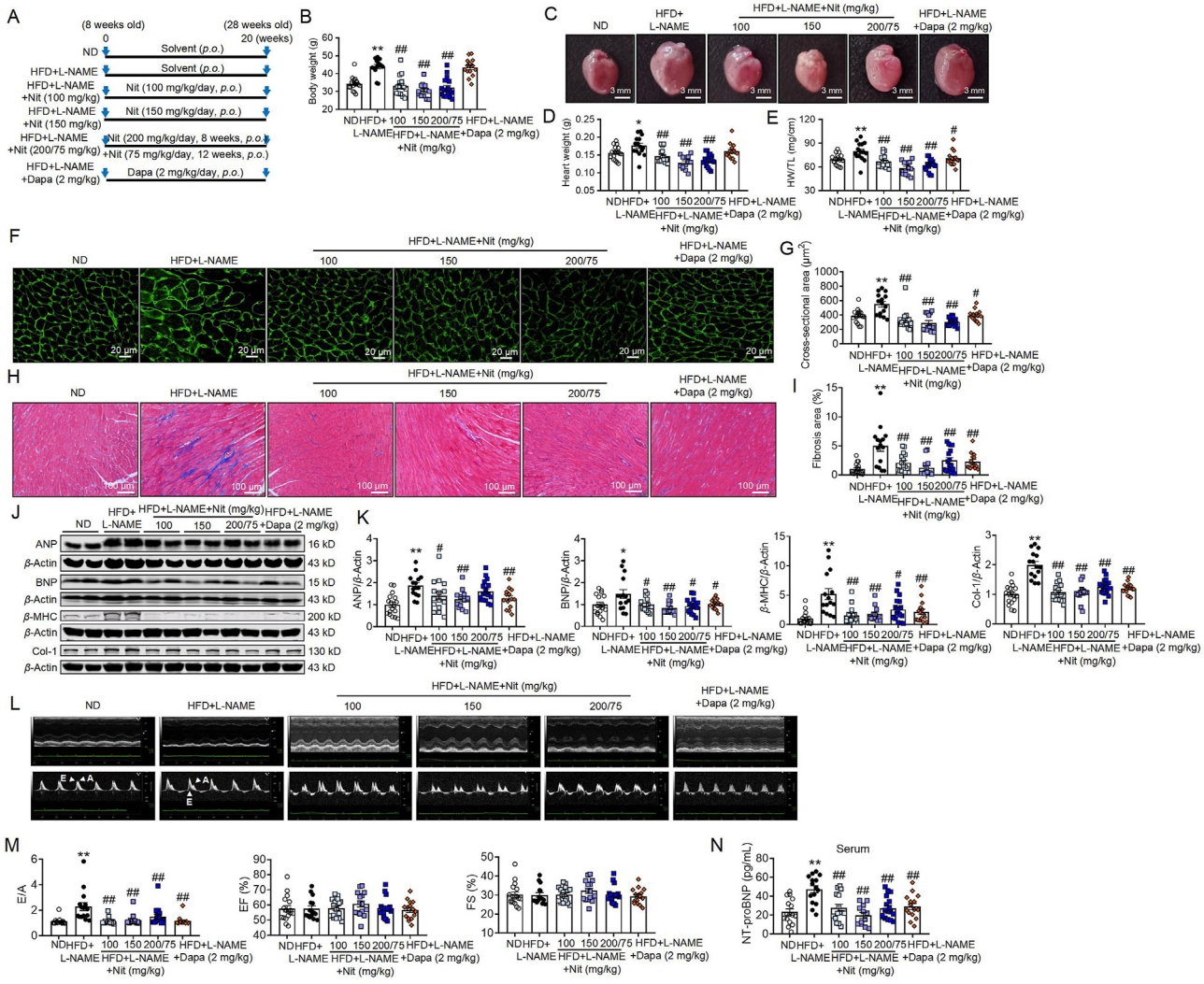

Figure 1 Oral nitazoxanide prevents HFD + L-NAME-induced cardiac hypertrophy, cardiac fibrosis and cardiac diastolic dysfunction in mice. (A) Diagram of the experimental design. (B) The data of body weight at the experiment termination. (C−E) Nitazoxanide inhibited HFD + L-NAME-induced the increase of heart weight and heart weight/tibia length (HW/TL) in mice. The representative images of hearts are shown in (C). (F, G) Nitazoxanide inhibited HFD + L-NAME-induced the increase of cardiomyocyte cross-sectional area in mice. The representative images of WGA staining of hearts are shown in (F) and the analyzed data of cardiomyocyte cross-sectional area are shown in (G). (H, I) Nitazoxanide inhibited HFD + L-NAME-induced the increase of cardiac collagen deposition in mice. The representative images of Masson's trichrome staining of hearts are shown in (H) and the analyzed data of cardiac fibrosis area are shown in (I). (J, K) Nitazoxanide reduced the levels of ANP, BNP, β-MHC and collagen-1 in heart tissues from HFD + L-NAME induced mice. The representative images of Western blot bands are shown in (J) and the analyzed data are shown in (K). (L, M) Nitazoxanide improved HFD + L-NAME-induced heart diastolic dysfunction in mice. The representative images of echocardiography are shown in (L) and analyzed data of E/A, EF (%) and FS (%) are shown in (M). (N) Nitazoxanide inhibited HFD + L-NAME-induced the increase of NT-proBNP in serum. Data are expressed as mean ± SEM. $n = 12-17$. $^{**}P < 0.01$ *vs.* ND; $^{\#}P < 0.05$, $^{\#\#}P < 0.01$ *vs.* HFD + L-NAME. HFD, high-fat diet; ND, normal diet; Nit, nitazoxanide; Dapa, dapagliflozin; E/A, ratio between mitral E wave and A wave; EF, ejection fraction; FS, fractional shortening; NT-proBNP, N-terminal pro-brain natriuretic peptide.

HFD + L-NAME-induced increases of serum TC and LDL-C levels (Fig. 3E and F).

3.4. *Nitazoxanide improves the hepatic steatosis in HFD + L-NAME-treated mice*

In HFD + L-NAME "two-hit" mouse model, HFD feeding increases serum lipid levels and liver lipid accumulation; meanwhile, L-NAME treatment leads to endothelial dysfunction which promotes the pathogenesis and progression of metabolic-associated fatty liver disease[25]. In the present study, we found that HFD + L-NAME treatment induced significant hepatic steatosis in mice. As shown in Fig. 4A, the livers of HFD + L-NAME-treated mice were swollen and pale in color. Both liver weight and liver weight index (liver weight/tibial length) of HFD + L-NAME-treated mice significantly increased compared to that in ND group (Fig. 4B). However, the altered appearance of livers and the increased liver weight and liver weight index in HFD + L-NAME-treated mice were restored by nitazoxanide treatment (Fig. 4A and B). Nitazoxanide treatment also prevented

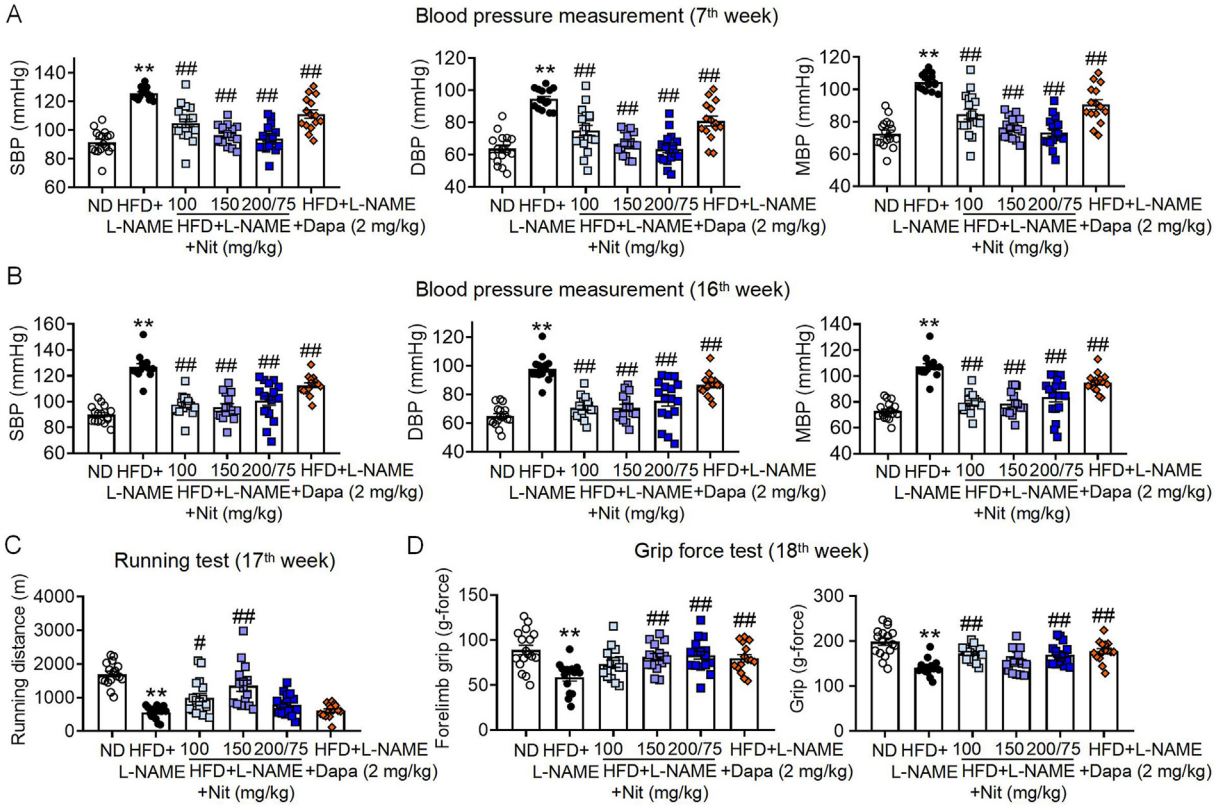

Figure 2 Oral nitazoxanide prevents HFD + L-NAME-induced increase of blood pressure and decrease of exercise tolerance in mice. (A, B) Nitazoxanide inhibited HFD + L-NAME-induced increase of systolic blood pressure (SBP), diastolic blood pressure (DBP) and mean blood pressure (MBP) in mice at the 7th (A) and 16th weeks (B). (C, D) Nitazoxanide improved the decrease of exercise tolerance induced by HFD + L-NAME in mice. The analyzed data of running distance at the 17th week are shown in (C) and the analyzed data of forelimb grip and limb grip at the 18th week are shown in (D). Data are expressed as mean ± SEM, $n = 15-18$. $^{**}P < 0.01$ *vs.* ND; $^{\#}P < 0.05$, $^{\#\#}P < 0.01$ *vs.* HFD + L-NAME. HFD, high-fat diet; ND, normal diet; Nit, nitazoxanide; Dapa, dapagliflozin.

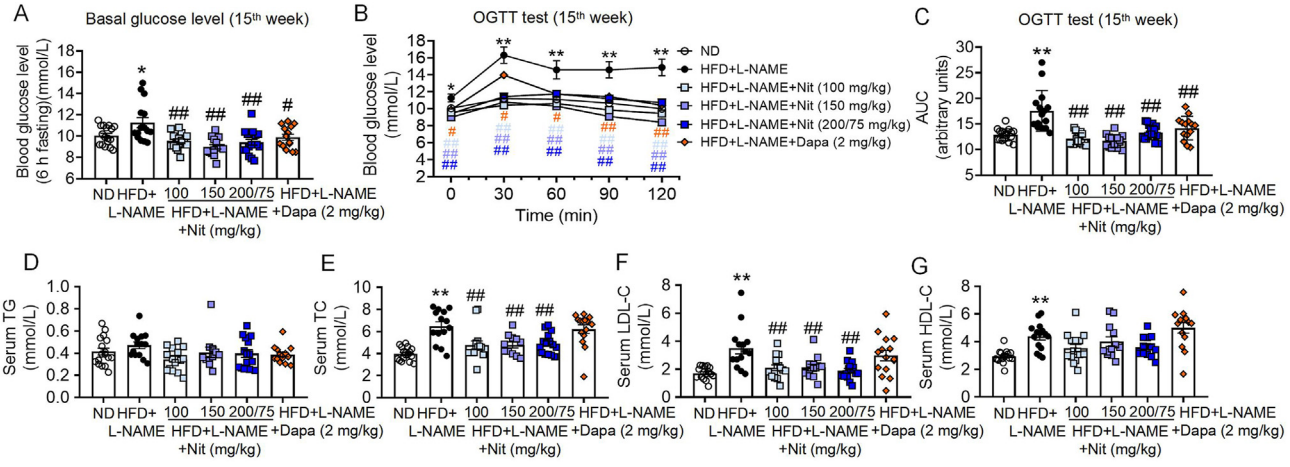

Figure 3 Oral nitazoxanide improves the impaired glucose handling and serum lipid disorders in HFD + L-NAME-treated mice. (A) Nitazoxanide inhibited the increase of 6-h fasting blood glucose induced by HFD + L-NAME in mice. (B, C) Nitazoxanide improved HFD + L-NAME-induced glucose handling impairment in mice. The statistical data of the oral glucose tolerance test (OGTT) are shown in (B) and the area under the time-blood glucose curve (AUC) of the OGTT was shown in (C). (D−G) Nitazoxanide improved serum lipid disorders induced by HFD + L-NAME in mice. The serum lipid indicators included triglyceride (TG) (D), total cholesterol (TC) (E), LDL-C (F) and HDL-C (G). Data are expressed as mean ± SEM, $n = 11-17$. $^{*}P < 0.05$, $^{**}P < 0.01$ *vs.* ND; $^{\#}P < 0.05$, $^{\#\#}P < 0.01$ *vs.* HFD + L-NAME. HFD, high-fat diet; ND, normal diet; Nit, nitazoxanide; Dapa, dapagliflozin; LDL-C, low-density lipoprotein cholesterol; HDL-C, high-density lipoprotein cholesterol.

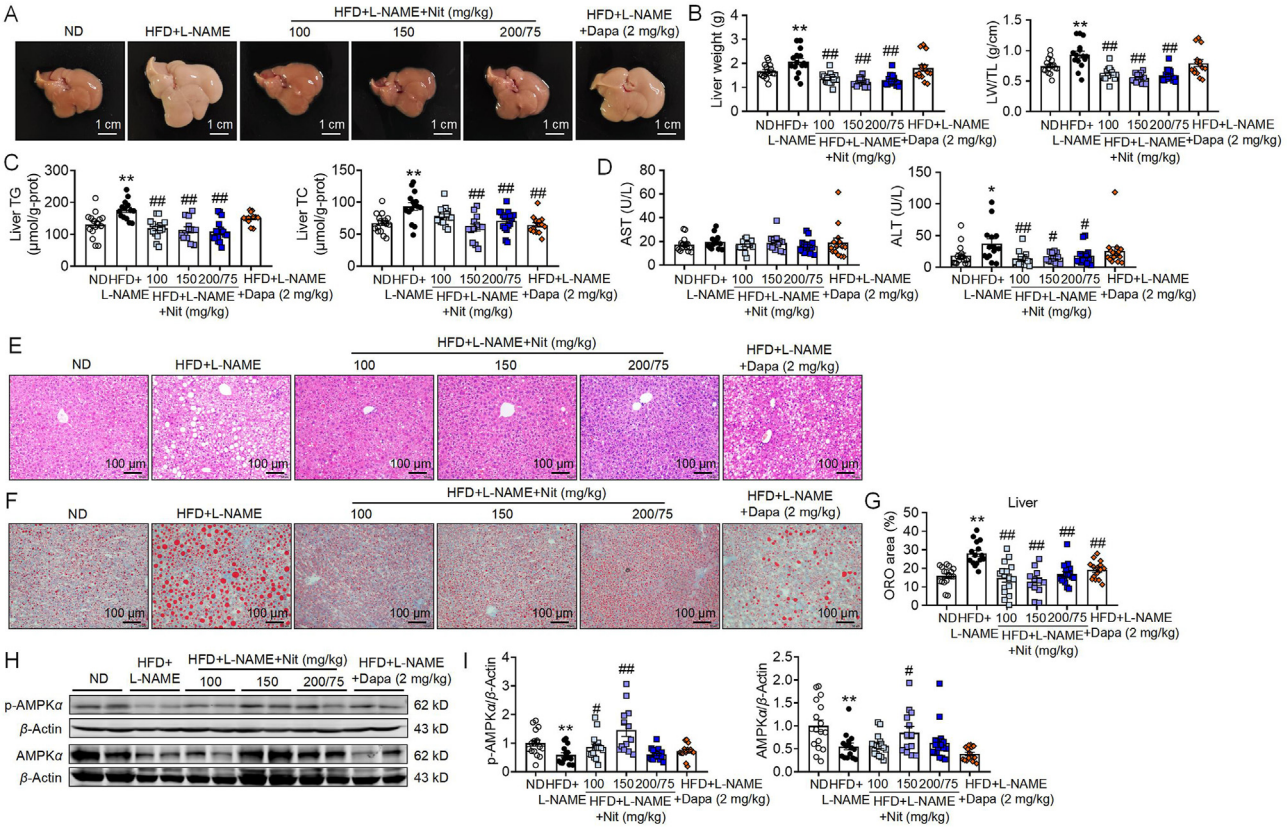

Figure 4 Oral nitazoxanide improves the hepatic steatosis of HFD + L-NAME-treated mice. (A) The representative images of livers showed that the livers of HFD + L-NAME-treated mice were swollen and pale in color and the altered appearance of livers were restored by nitazoxanide. (B) Nitazoxanide inhibited the increase of liver weight and liver weight/tibia length (LW/TL) induced by HFD + L-NAME in mice. (C) Nitazoxanide inhibited the increase of triglyceride (TG) and total cholesterol (TC) in livers induced by HFD + L-NAME in mice. (D) The serum levels of ALT and AST. (E) The representative images of H&E staining of livers. (F, G) The liver lipid deposits induced by HFD + L-NAME were improved by nitazoxanide. The representative images of Oil Red O (ORO) staining of livers are shown in (F) and the analyzed data of lipid deposits are shown in (G). (H, I) The representative images of Western blot bands and analyzed data showed that nitazoxanide increased the level of p-AMPKα and AMPKα in livers. Data are expressed as mean ± SEM, $n = 11-17$. $^{*}P < 0.05$, $^{**}P < 0.01$ *vs.* ND; $^{\#}P < 0.05$, $^{\#\#}P < 0.01$ *vs.* HFD + L-NAME. HFD, high-fat diet; ND, normal diet; Nit, nitazoxanide; Dapa, dapagliflozin; AST, aspartate aminotransferase; ALT, alanine transaminase.

the increases of liver TG, TC levels and serum ALT levels induced by HFD + L-NAME (Fig. 4C and D).

The livers of HFD + L-NAME-treated mice exhibited histopathological changes. Hematoxylin-eosin (H&E) staining of liver paraffin sections revealed significant hydropic degeneration of hepatocytes and macrovesicular steatosis in the livers of HFD + L-NAME-treated mice (Fig. 4E). The liver lipid deposits were further confirmed by Oil red O staining (Fig. 4F and G). The above pathological characteristics induced by HFD + L-NAME were significantly improved by nitazoxanide treatment (Fig. 4E−G). Dapagliflozin, a positive drug for HFpEF therapy, reduced HFD + L-NAME-induced increase of liver TC (Fig. 4C). Nevertheless, dapagliflozin did not improve HFD + L-NAME-induced increases of liver TG and serum ALT and pathological changes (Fig. 4C−E). Comprehensively, dapagliflozin-induced improvement of lipid metabolism disorders was inferior to that of nitazoxanide in mice.

AMPK activation has been the target for regulating carbohydrate and lipid metabolism disorders[26]. Our previous study had shown that nitazoxanide treatment activated AMPK in mouse livers *in vivo*[11]. Here, we assessed the AMPK protein expression and activity in liver tissues of mice from different groups. As shown in Fig. 4H and I, nitazoxanide treatment increased the inhibited AMPK activity induced by HFD + L-NAME.

3.5. *Nitazoxanide reduces the fat depots in HFD + L-NAME-treated mice*

Obesity contributes to the development of cardiovascular diseases, type 2 diabetes, and liver diseases etc.[27]. HFD + L-NAME "two-hit" induces a significant increase in white adipose tissue in several depots, including subcutaneous white adipose tissues (sWATs), perirenal white adipose tissues (pWATs) and epididymal white adipose tissues (eWATs). These increases were manifested not only as weight increase but also as enlargement of adipocyte size (Fig. 5). Nitazoxanide treatment significantly inhibited HFD + L-NAME-induced increases of weight and adipocyte size of sWATs, pWATs and eWATs (Fig. 5). Dapagliflozin treatment showed no significant effect on HFD + L-NAME-induced increases of sWATs, pWATs and eWATs weight, though the adipocyte sizes of sWATs, pWATs and eWATs in mice of HFD + L-NAME + Dapa group were statistically smaller than that of HFD + L-NAME group (Fig. 5).

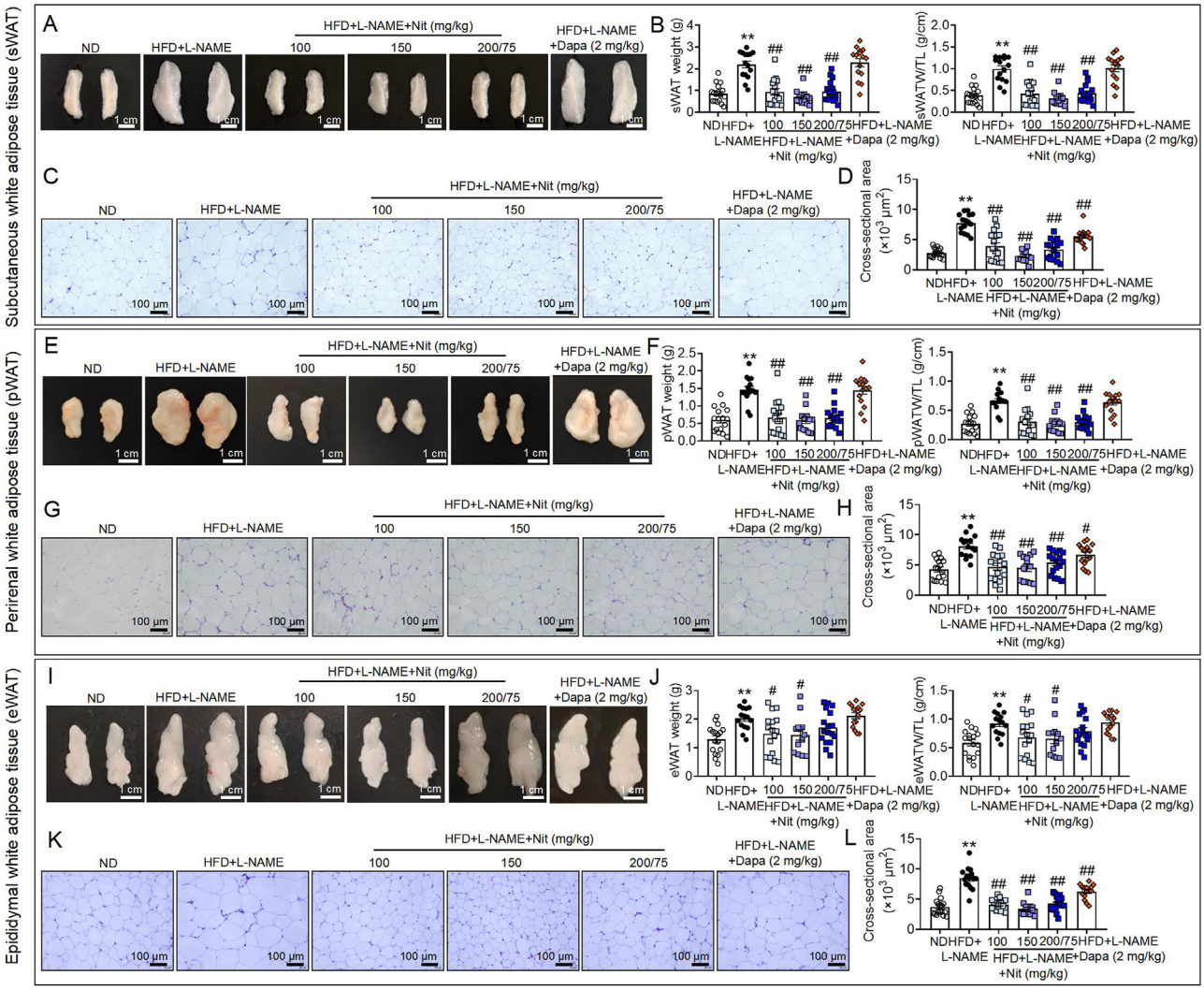

Figure 5 Oral nitazoxanide reduces the fat depots of HFD + L-NAME-treated mice. Nitazoxanide not only inhibited HFD + L-NAME-induced increases of weight of sWATs (A, B), pWATs (E, F) and eWATs (I, J) but also the adipocyte size of sWATs (C, D), pWATs (G, H) and eWATs (K, L). The representative images of H&E staining of sWATs, pWATs and eWATs are shown in (C, G and K). The analyzed data of the cross-sectional area of sWATs, pWATs and eWATs are shown in (D, H and L). Data are expressed as mean ± SEM, $n = 13-17$. $^{**}P < 0.01$ *vs.* ND; $^{\#}P < 0.05$, $^{\#\#}P < 0.01$ *vs.* HFD + L-NAME. sWATW/TL, the ratio of subcutaneous white adipose tissues weight to tibial length; pWATW/TL, the ratio of perirenal white adipose tissues weight to tibial length; eWATW/TL, the ratio of epididymal white adipose tissues weight to tibial length; HFD, high-fat diet; ND, normal diet; Nit, nitazoxanide; Dapa, dapagliflozin.

3.6. Nitazoxanide improves kidney fibrosis in HFD + L-NAME-treated mice

HFpEF and renal impairment coexist and they interact with each other in a feedback cycle to accelerate the progression of cardiorenal syndrome[28,29]. Kidney fibrosis has been reported in the SAUNA (an acronym for salty drinking water, unilateral nephrectomy and chronic aldosterone) HFpEF mouse model[28]. In the present study, although there was no difference in the kidney weight, ratio of kidney weight to tibial length (KW/TL), and kidney lipid deposition (elevated by Oil red O staining) among the groups (Supporting Information Figs. S3A and S3B), significant kidney fibrosis was detected in HFD + L-NAME-treated mice. H&E staining showed abnormal extracellular matrix and Masson's trichrome staining revealed glomerular, periglomerular and interstitial fibrosis in the kidneys of HFD + L-NAME-treated mice ((Figs. S3C and S3D). The analyzed data of fibrotic area were shown in Fig. S3E. These results were consistent with the increased collagen-1 protein level in the kidney of HFD + L-NAME-treated mice (Figs. S3F and S3G). Nitazoxanide treatment significantly inhibited HFD + L-NAME-induced kidney fibrosis (Figs. S3D–S3G). Dapagliflozin treatment inhibited HFD + L-NAME-induced increase of collagen-1 expression but did not show inhibitory effect on collagen deposition as evaluated by Masson's trichrome staining (Figs. S3D–S3G).

3.7. Nitazoxanide is therapeutic in established HFpEF and metabolic syndrome induced by HFD + L-NAME in mice

The above results demonstrated that oral nitazoxanide prevented HFpEF phenotypes and metabolic syndrome in mice under the conditions of simultaneous treatment with HFD + L-NAME and

drugs. We wondered whether nitazoxanide was therapeutic in established HFpEF and metabolic syndrome models. Therefore, firstly, we treated mice with HFD + L-NAME for seven weeks to establish the HFpEF model (Supporting Information Fig. S4A). The echocardiography results showed that the E/A ratio but not EF (%) and FS (%) increased in mice treated with HFD + L-NAME for 7 weeks (Figs. S4B and S4C), and the systolic blood pressure, diastolic blood pressure and mean blood pressure also increased in the HFD + L-NAME-treated mice (Fig. S4D). We thought that the HFpEF model was successfully established. A previous study reported that the HFpEF model could be established by HFD + L-NAME treatment for 5 weeks[21].

Next, the HFD + L-NAME-treated mice were randomly divided into three groups, HFD + L-NAME, HFD + L-NAME + Nit (150 mg/kg), HFD + L-NAME + Dapa (2 mg/kg), and were treated for a further 9 weeks (Fig. 6A). As shown in Fig. 6B−E, nitazoxanide and dapagliflozin treatments inhibited HFD + L-NAME-induced increases of body weight, heart weight and the ratio of heart weight to tibial length. The inhibitory effect of nitazoxanide and dapagliflozin treatments on HFD + L-NAME-induced heart hypertrophy was further confirmed by WGA staining (Fig. 6F and G) and quantitative assessment of ANP, BNP, β-MHC protein levels in heart tissues (Fig. 6H and I). HFD + L-NAME-induced cardiac fibrosis was also mitigated by nitazoxanide and dapagliflozin treatments (Fig. 6J and K). Echocardiography results showed that E/A ratio but not EF (%) and FS (%) increased in HFD + L-NAME-treated mice and the increase was inhibited by nitazoxanide and dapagliflozin treatments, which was parallel to the result of serum NT-proBNP level (Fig. 6L−N). Other echocardiographic parameters were shown in Supporting Information Fig. S5.

At the 15th week, we measured systolic blood pressure (SBP), diastolic blood pressure (DBP) and mean blood pressure (MBP) of mice. As shown in Fig. 7A−C, nitazoxanide and dapagliflozin treatments reduced HFD + L-NAME-induced increases of SBP, DBP and MBP. At the 16th week, we measured the running tolerance and grip force of mice. As shown in Fig. 7D and E, nitazoxanide and dapagliflozin treatments rescued the decreased exercise tolerance induced by HFD + L-NAME.

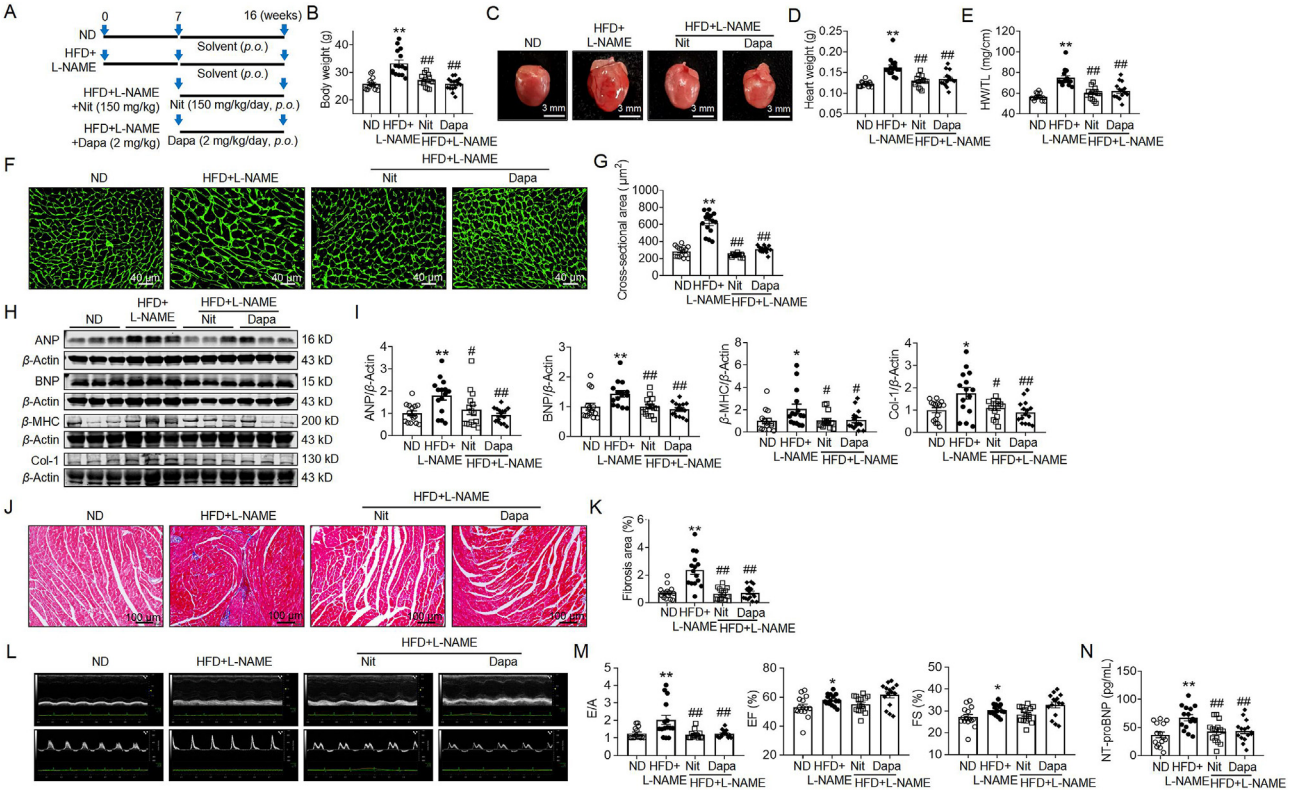

Figure 6 Oral nitazoxanide rescues cardiac hypertrophy, cardiac fibrosis and cardiac diastolic dysfunction in the established HFD + L-NAME-induced mouse model. (A) Diagram of the experimental design. (B) The data of body weight at the experiment termination. (C−E) Nitazoxanide reduced the increase of heart weight and heart weight/tibia length (HW/TL) in the established HFD + L-NAME-induced mouse model. The representative images of hearts are shown in (C). (F, G) Nitazoxanide rescued the increase of cardiomyocyte cross-sectional area in the established HFD + L-NAME-induced mouse model. The representative images of WGA staining of hearts are shown in (F) and the analyzed data of cardiomyocyte cross-sectional area are shown in (G). (H, I) Nitazoxanide reduced the levels of ANP, BNP, β-MHC and collagen-1 in heart tissues. The representative images of Western blot bands are shown in (H) and the analyzed data are shown in (I). (J, K) Nitazoxanide inhibited the increase of cardiac collagen deposition in the established HFD + L-NAME-induced mouse model. The representative images of Masson's trichrome staining of hearts are shown in (J) and the analyzed data of cardiac fibrosis area are shown in (K). (L, M) Nitazoxanide improved heart diastolic dysfunction in the established HFD + L-NAME-induced mouse mode. The representative images of echocardiography are shown in (L) and analyzed data of E/A, EF (%) and FS (%) are shown in (M). (N) Nitazoxanide inhibited the increase of NT-proBNP in serum. Data are expressed as mean ± SEM, $n = 15$. $^{*}P < 0.05$, $^{**}P < 0.01$ *vs.* ND; $^{\#}P < 0.05$, $^{\#\#}P < 0.01$ *vs.* HFD + L-NAME. HFD, high-fat diet; ND, normal diet; Nit, nitazoxanide; Dapa, dapagliflozin; E/A, ratio between mitral E wave and A wave; EF, ejection fraction; FS, fractional shortening; NT-proBNP, N-terminal pro-brain natriuretic peptide.

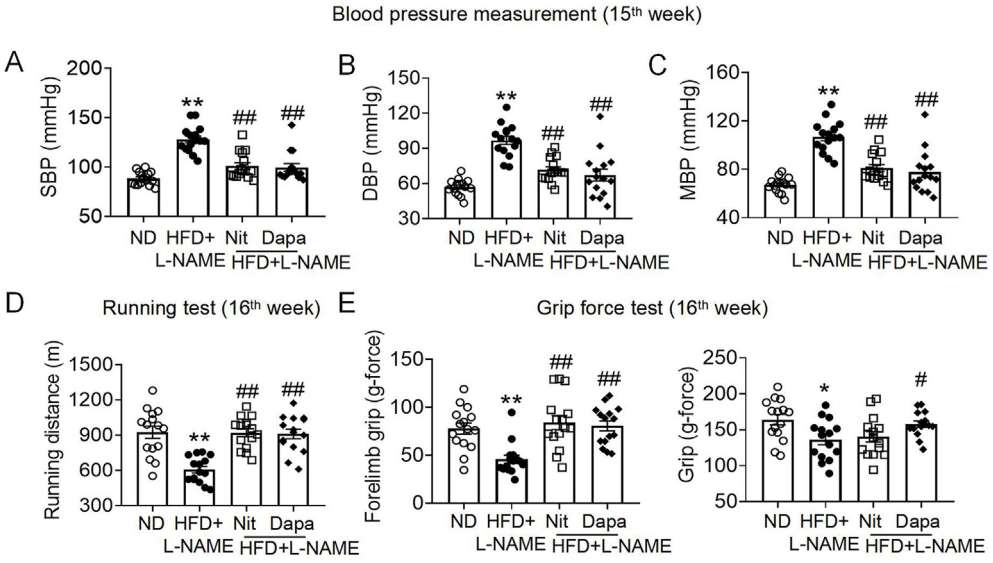

Figure 7 Oral nitazoxanide reverses the increased blood pressure and the impaired exercise tolerance in the established HFD + L-NAME-induced mouse model. (A−C) Nitazoxanide inhibited the increase of systolic blood pressure (SBP), diastolic blood pressure (DBP) and mean blood pressure (MBP) in the established HFD + L-NAME-induced mouse model. (D, E) Nitazoxanide improved the decrease of exercise tolerance in the established HFD + L-NAME-induced mouse model. The analyzed data of running distance at the 16th week are shown in (D) and the analyzed data of forelimb grip and limb grip at the 16th week are shown in (E). Data are expressed as mean ± SEM, $n = 15$. $^{*}P < 0.05$, $^{**}P < 0.01$ *vs.* ND; $^{\#}P < 0.05$, $^{\#\#}P < 0.01$ *vs.* HFD + L-NAME. HFD, high-fat diet; ND, normal diet; Nit, nitazoxanide; Dapa, dapagliflozin.

Nitazoxanide and dapagliflozin treatments reduced HFD + L-NAME-induced increases of liver weight, liver weight index (liver weight/tibial length), liver TC and TG, and serum ALT in mice (Fig. 8A−D). Nitazoxanide and dapagliflozin treatments also improved HFD + L-NAME-induced hydropic degeneration of hepatocytes and liver lipid deposits (Fig. 8E−G). Nitazoxanide treatment restored the inhibited AMPK activity in liver tissues induced by HFD + L-NAME (Fig. 8H and I).

We performed the OGTT at the 15th week post-treatment. Nitazoxanide and dapagliflozin reduced 6-h fasting glucose levels and reversed the HFD + L-NAME-induced glucose handling impairment (Supporting Information Fig. S6A−S6C). Nitazoxanide and dapagliflozin treatments reduced the HFD + L-NAME-induced increases of serum TC, LDL-C and HDL-C levels (Fig. S6D−S6G). Additionally, nitazoxanide and dapagliflozin treatments reduced HFD + L-NAME-induced increases of the weight, weight index and adipocyte size of sWATs, pWATs and eWATs (Supporting Information Fig. S7).

Nitazoxanide and dapagliflozin had no effect on the HFD + L-NAME-induced increases of kidney weight and kidney weight index (kidney weight/tibial length) (Supporting Information Fig. S8A) but mitigated the abnormal extracellular matrix and fibrosis in the glomerular, periglomerular and interstitial areas of the kidney (Fig. S8B−S8E). These results were further validated by the measurement of collagen-1 protein levels in the kidney tissues (Fig. S8F and S8G).

3.8. *Tizoxanide increases basal mitochondria metabolism of cardiomyocytes*

Our previous studies have demonstrated that nitazoxanide and tizoxanide induced mitochondrial uncoupling, and based on the mitochondrial uncoupling mechanism, nitazoxanide was proven to improve experimental hyperlipidemia and hepatic steatosis, inhibit atherosclerosis, inhibit NLRP3 inflammasome activation, improve aging, and inhibit fibrosis response[8,11,12,14,30]. Actually, all the above-mentioned effects of nitazoxanide are the potential mechanisms of nitazoxanide against HFpEF. Additionally, we further explored the effect of tizoxanide, the *in vivo* active metabolite of nitazoxanide, on mitochondria respiration of cardiomyocytes. As shown in Fig. 9A and B, tizoxanide concentration-dependently increased oxygen consumption rate (OCR) of cultured primary cardiomyocytes when oligomycin was used to inhibit ATP synthase, indicating that tizoxanide induced increase of leak respiration of cardiomyocytes. However, tizoxanide treatment increased the basal mitochondria respiration but did not increase the mitochondrial ATP production in cardiomyocytes (Fig. 9C and D), indicating that tizoxanide increased basal energy consumption. Furthermore, we found that the mitochondrial complex I, complex II, and complex IV activities increased in mouse heart tissues under the presence of tizoxanide (Fig. 9E and F). These results indicated that tizoxanide increased the basal mitochondria metabolism of cardiomyocytes indeed. Fatty acids are the major substrates for energy provision in hearts, but lipid accumulation contributes to the pathogenesis of HFpEF[13,31]. We thought that tizoxanide-induced increase of basal metabolism of cardiomyocytes would consume lipids, thus improving lipid accumulation in hearts. We further measured the triglyceride content in heart tissues from the preventive experiments (Fig. 1A). As shown in Fig. 9G, the triglyceride content in heart tissues from HFD + L-NAME-treated mice increased, and the increases were reduced by both nitazoxanide and dapagliflozin treatments. These results demonstrated that nitazoxanide could improve lipid accumulation in hearts, which might partly contribute to the protective effect of nitazoxanide against HFpEF.

3.9. *Tizoxanide inhibits cardiomyocyte hypertrophy and collagen-1 secretion from cardiac fibroblasts in vitro*

Mitochondrial uncoupling induces AMPK activation, and inhibits Akt and STAT3 activation[8,11,32]. Activation of AMPK or

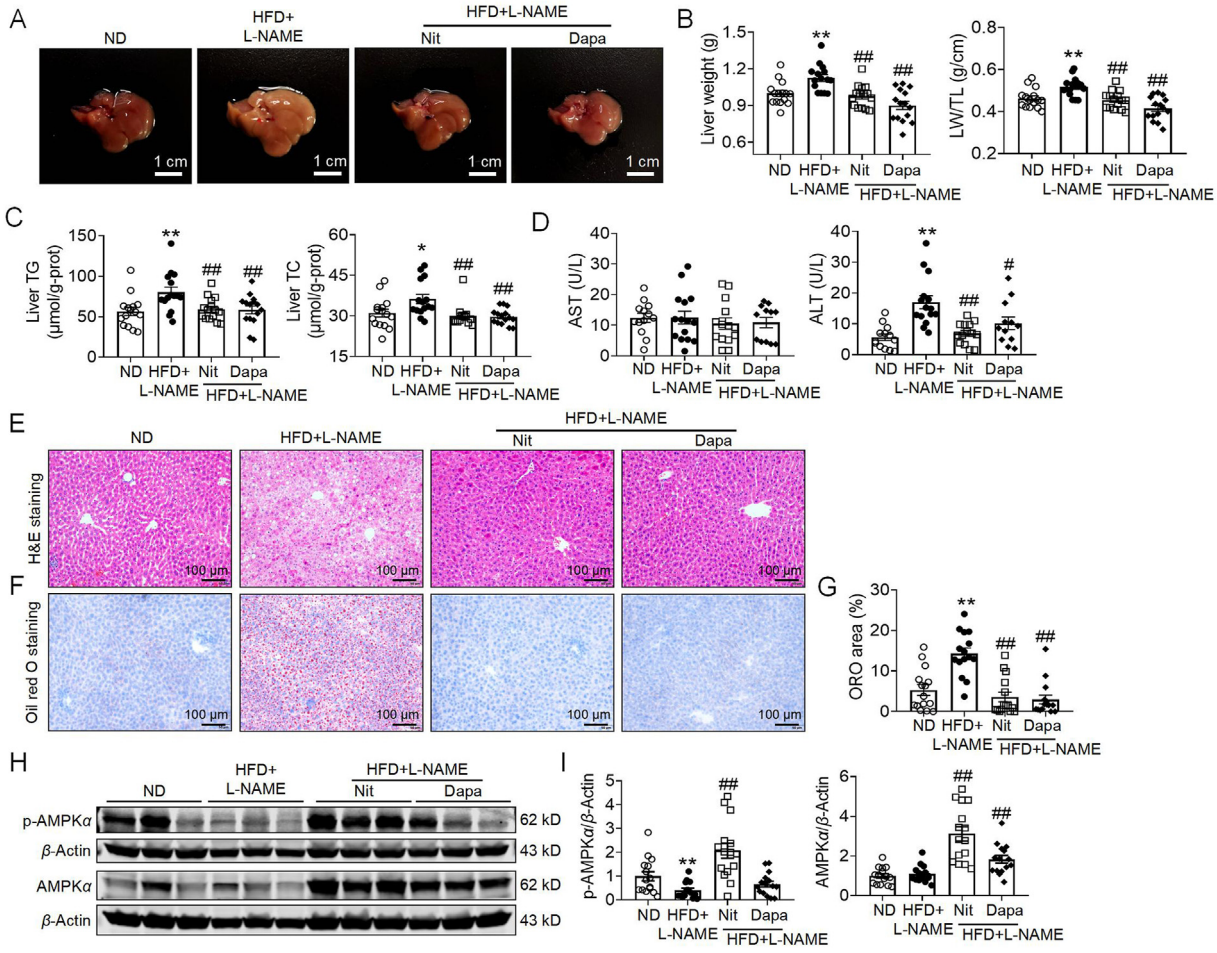

Figure 8 Oral nitazoxanide improves hepatic steatosis in an established HFD + L-NAME-induced mouse model. (A) The representative images of livers showed that the livers of HFD + L-NAME-treated mice were swollen and pale in color and the altered appearance of livers were restored by nitazoxanide. (B) Nitazoxanide inhibited the increase of liver weight and liver weight/tibia length (LW/TL) in the established HFD + L-NAME-induced mouse model. (C) Nitazoxanide inhibited the increase of triglyceride (TG) and total cholesterol (TC) in the established HFD + L-NAME-induced mouse model. (D) The serum levels of ALT and AST. (E) The representative images of H&E staining of livers. (F, G) The liver lipid deposits induced by HFD + L-NAME were improved by nitazoxanide. The representative images of Oil Red O (ORO) staining of livers are shown in (F) and the analyzed data of lipid deposits are shown in (G). (H, I) The representative images of Western blot bands and analyzed data showed that nitazoxanide increased the level of p-AMPKα and AMPKα in livers. Data are expressed as mean ± SEM, $n = 12-15$. $^{*}P < 0.05$, $^{**}P < 0.01$ *vs.* ND; $^{\#}P < 0.05$, $^{\#\#}P < 0.01$ *vs.* HFD + L-NAME. HFD, high-fat diet; ND, normal diet; Nit, nitazoxanide; Dapa, dapagliflozin; AST, aspartate aminotransferase; ALT, alanine transaminase.

inhibition of Akt and STAT3 inhibits heart hypertrophy[33-36]. Phenylephrine (PE), an inducer of heart hypertrophy, has been demonstrated to induce heart hypertrophy through activating STAT3 and Akt signals[37,38]. We tested the effect of tizoxanide on PE-induced cardiomyocyte hypertrophy *in vitro*. Results showed that tizoxanide treatment significantly inhibited PE-induced cardiomyocyte hypertrophy (Supporting Information Fig. S9A−S9D). Tizoxanide treatment activated AMPK of cultured cardiomyocytes in presence of PE (Fig. S9E and S9F). PE treatment activated STAT3 and Akt signals which was inhibited by tizoxanide treatment (Fig. S9E and S9F). We further detected the AMPK, Akt, and STAT3 signals in heart tissues from the *in vivo* experiments as shown in Fig. 1A. Results show that oral nitazoxanide activated the inhibited AMPK, and inhibited the activated Akt and STAT3 in heart tissues of mice treated with HFD + L-NAME (Supporting Information Fig. S10), which was consistent with results of *in vitro* experiments (Fig. S9E and S9F). These results indicated that the inhibitory effect of nitazoxanide on cardiomyocyte hypertrophy might be through activating AMPK and inhibiting STAT3 and Akt signals.

JAK/STAT3 activation is crucial in cardiac fibrosis[39]. We found that tizoxanide treatment also significantly inhibited STAT3 signal in normal cultured cardiac fibroblasts (Supporting Information Fig. S11A and S11B) and IL-6-stimulated cardiac fibroblasts (Fig. S11C and S11D). Since IL-6/STAT3 activation causes cardiac fibrosis, we examined the effect of tizoxanide on collagen secretion of cardiac fibroblasts. Results show that tizoxanide treatment inhibited collagen-1 secretion from normal cultured cardiac fibroblasts or IL-6-, TGF-β1-stimulated cardiac fibroblasts (Fig. S11E−S11J).

3.10. Tizoxanide relaxes the constricted artery and pretreatment of tizoxanide inhibits artery constriction ex vivo

Our previous studies demonstrate that mitochondrial uncouplers share common effect of vasorelaxation[3,4,6]. Mesenteric arteries are

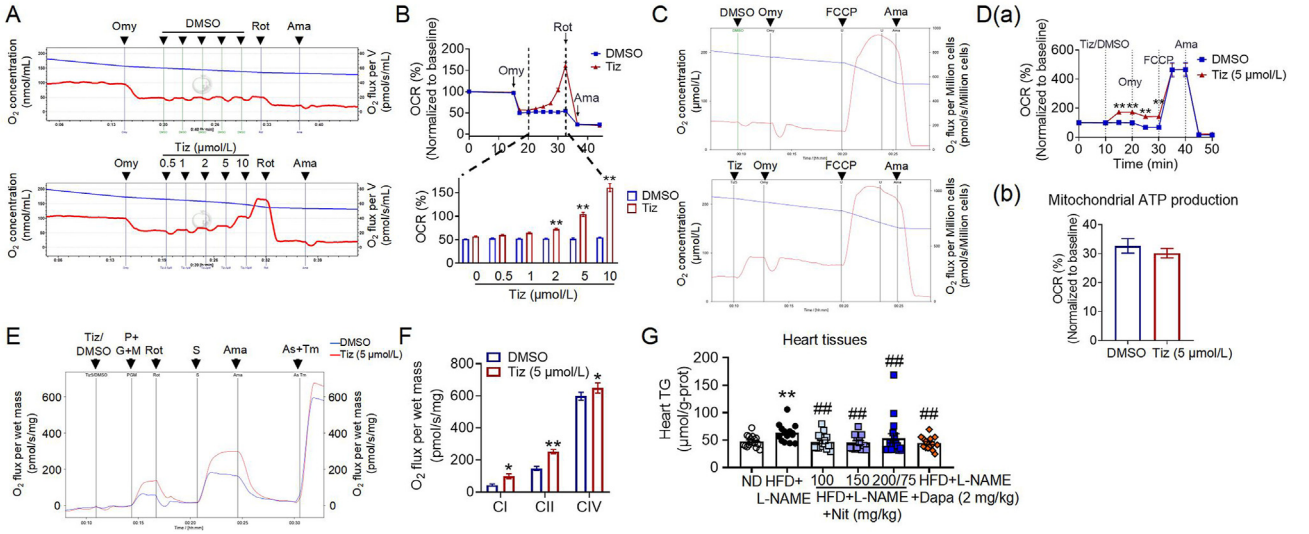

Figure 9 Tizoxanide increases basal mitochondria metabolism of cardiomyocytes and oral nitazoxanide reduces the triglyceride content in heart tissues of HFD + L-NAME-treated mice. (A, B) Tizoxanide concentration-dependently increased oxygen consumption rate (OCR) of cultured primary cardiomyocytes after ATP synthase was inhibited by oligomycin. The representative original recordings are shown in (A) and the analyzed data of oxygen consumption rate (OCR) are shown in (B). $n = 6$ in each group. (C, D) Tizoxanide treatment increased the basal mitochondria respiration but did not increase the mitochondrial ATP production in cardiomyocytes. The difference of OCR value before and after Omy treatment represented mitochondrial ATP production. The representative original recordings are shown in (C) and the analyzed data of OCR (a) and mitochondrial ATP production (b) are shown in D. $n = 7$ in each group. (E, F) Tizoxanide treatment increased mitochondrial complex I, complex II, and complex IV activities in mouse heart tissues. The representative original recordings are shown in (E) and the analyzed data of O_2 flux per wet mass (pmol/s/mg) are shown in (F). $n = 7$ in each group. Data are expressed as mean ± SEM. $^{*}P < 0.05$, $^{**}P < 0.01$ *vs.* DMSO (control). (G) The contents of heart triglyceride (TG) in heart tissues. Data are expressed as mean ± SEM, $n = 13-17$. $^{**}P < 0.01$ *vs.* ND; $^{\#\#}P < 0.01$ *vs.* HFD + L-NAME. Omy, oligomycin; Rot, rotenone; Ama, antimycin A; P, pyruvic acid; G, glutamic acid; M, malic acid; S, succinic acid; As, ascorbic acid; Tm, *N*,*N*,*N*′,*N*′-tetramethyl-*p*-phenylenediamine dihydrochloride; Tiz, Tizoxanide; Nit, nitazoxanide; Dapa, dapagliflozin; HFD, high-fat diet; ND, normal diet.

resistance arteries and play an important role in regulating blood pressure. The above results showed that oral nitazoxanide reduced HFD + L-NAME-induced increase of blood pressure, therefore, we further examined the effect of tizoxanide on vasoconstriction and vasorelaxation of rat mesenteric arteries *ex vivo*. Tizoxanide as a mitochondrial uncoupler, induced concentration-dependent relaxation in both endothelium-intact and endothelium-denuded rat mesenteric arteries precontracted with PE (Fig. 10A) and thromboxane A2 analog U46619 (Fig. 10B). Tizoxanide pre-treatment inhibited PE (Fig. 10C and D) and U46619 (Fig. 10E and F)-induced constriction of rat mesenteric arteries with intact and denuded endothelium in a concentration-dependent manner. This direct effect might be the potential mechanism of the effect of nitazoxanide on blood pressure *in vivo* in HFpEF model.

Furthermore, we attempted to assess the relaxation function of the thoracic aorta of mice from different groups in the *in vivo* experiments (Fig. 1A). We found that the contractile response of the mouse thoracic aorta to PE and the relaxation response to ACh was almost undetectable in mice from ND (Fig. 10G(a)) or HFD + L-NAME group (data not shown), whereas these thoracic aortae were responsive to KPSS stimulation (Fig. 10G(b)). We compared the contractile response of the thoracic aorta to PE and KPSS stimuli between young (8 weeks old) and old (28 weeks old) mice. In contrast to the old mice (28 weeks old) (Fig. 10G(a−b)), the thoracic aorta from young mice (8 weeks) exhibited significant contraction after PE and KPSS treatments (Fig. 10H). These results indicated that PE-induced contractile function of the thoracic aorta from old mice was impaired, and the reduced response of thoracic aorta to PE in HFD + L-NAME-treated mice might be associated with aging. We further compared the KPSS-induced contraction of thoracic aorta in mice from different groups. Results showed that the KPSS-induced thoracic aorta contraction of mice in HFD + L-NAME group was decreased, and the decrease was restored by nitazoxanide and dapagliflozin treatments (Fig. 10I and J).

4. Discussion

HFpEF is a systemic and complex clinical syndrome associated with a wide range of risk factors such as aging, hypertension, metabolic syndrome, obesity, diabetes mellitus, hyperlipidemia, and renal diseases. The pathogenetic mechanism of HFpEF is so complicated that it poses a challenge to the development of pre-clinical HFpEF models mimicking the clinical phenotypes. Currently, several multifactorial HFpEF mouse models have been developed, such as the deoxycorticosterone acetate salt-sensitive model, aldosterone uninephrectomy model, HFD and L-NAME "two-hit" model, HFD and angiotensin II infusion "two-hit" model, aging, HFD and angiotensin II infusion "three-hit" model, aging, HFD and desoxycorticosterone pivalate "three-hit" model[40]. Schiattarella et al.[13] and Solomon et al.[21] developed a HFD and L-NAME "two-hit" mouse model resembling human HFpEF. In this model, HFD feeding increased body weight and induced glucose intolerance, while L-NAME treatment raised both systolic and diastolic blood pressure[21]. We applied this "two-hit" model to evaluate the effect of nitazoxanide on HFpEF and metabolic syndrome in mice. Nitazoxanide, an FDA-approved

antiprotozoal drug, has been reported to improve type 2 diabetes mellitus in rats[41]. Our previous studies have demonstrated that nitazoxanide improved hyperlipidemia and hepatic steatosis, inhibited inflammation, atherosclerosis and fibrosis, and exhibited an anti-aging effect in pre-clinical models[8,11,12,14]. Based on the known pathogenetic mechanism of HFpEF, we speculated that nitazoxanide would be protective against HFpEF. In this study, we proved that oral nitazoxanide significantly prevented HFD + L-NAME-induced HFpEF and metabolic syndrome in mice, and in the established HFpEF and metabolic syndrome in mice, delayed nitazoxanide treatment reversed the pathological phenotypes.

4.1. *Comprehensive mechanisms of the effects of nitazoxanide*

Nitazoxanide is rapidly hydrolyzed to tizoxanide after absorption *in vivo*, only tizoxanide could be detected in the plasma. The C_{max} of tizoxanide after single- or multiple-dose oral administration of nitazoxanide (500 mg) in clinic was 9.05−10.6 μg/mL (about 34−40 μmol/L)[42]. In the present study, tizoxanide was used at 1, 2, 5 and 10 μmol/L concentrations in the *in vitro* experiments, which was clinically equivalent.

Nitazoxanide is a representative mitochondrial uncoupler. As a mitochondrial uncoupler, nitazoxanide offers a significant advantage in that it exerts a mitochondrial uncoupling effect not only *in vitro* but also *in vivo*[8,11,14]. The narrow therapeutic window and off-target effect are common defects of mitochondrial uncouplers. Although it has been reported that mitochondrial uncouplers protect against metabolic-associated fatty liver disease, insulin resistance, type 2 diabetes, atherosclerosis, aging, etc.[43-45], no drug based on the mitochondrial uncoupling mechanism has yet been approved in clinic. Our strategy is to find the drugs with mitochondrial uncoupling effect from the known FDA-approved clinical drugs, thus, it is more possible for the discovered drugs to be clinically translated based on the mitochondrial uncoupling mechanism. Our previous studies have demonstrated that both nitazoxanide and its active metabolite tizoxanide activated cellular AMPK, inhibited NLRP3 inflammasome activation, and oral nitazoxanide improved experimental hyperlipidemia, hepatic steatosis in hamsters and mice and inhibited atherosclerosis in mice[8,11]. Our latest work demonstrated that nitazoxanide and tizoxanide extended the lifespan and healthspan of *C. elegans* through AMPK/sir/Daf pathways[12]. We thought that all the effects of nitazoxanide as proven above contributed to the protection of nitazoxanide against HFpEF.

We further examined the direct effect of tizoxanide on cardiomyocyte mitochondrial respiration, cardiomyocyte hypertrophy, collagen secretion from cardiac fibroblasts, and rat mesenteric artery function *in vitro*. Since nitazoxanide is completely metabolized to the active metabolite tizoxanide *in vivo*, we studied the direct effect of tizoxanide *in vitro*. We found that tizoxanide induced increase of the basal mitochondria metabolism of cardiomyocytes. Since fatty acids are the major substrates for energy providing in hearts and lipid accumulation contributes to the pathogenesis of HFpEF[13,31], we further found both nitazoxanide and dapagliflozin treatments reduced the increased triglyceride content in heart tissues induced by HFD + L-NAME (Fig. 9G), indicating that the improvement of myocardial lipid accumulation might partly contribute to the protective effect of nitazoxanide against HFpEF.

Tizoxanide inhibited PE-induced cardiomyocyte hypertrophy, inhibited IL-6- and TGF-β1-induced collagen-1 secretion from cardiac fibroblasts, and relaxed PE- and U46619-induced constriction of rat mesenteric arteries. These direct actions may contribute to the beneficial effect of nitazoxanide on HFpEF and metabolic syndrome, especially in terms of inhibiting cardiac hypertrophy and cardiac fibrosis, and lowering blood pressure *in vivo*.

Aging, HFD diet or L-NAME treatment induces impairment of endothelium-dependent relaxation of arteries[46,47] and the impairment is closely associated with the development of hypertension. We attempted to assess the endothelium-dependent relaxation of the mouse aorta from all groups by using PE- and KPSS-induced vasoconstriction models. PE induces vasoconstriction by activating α1-adrenergic receptors on vascular smooth muscle cells, while KPSS induces vasoconstriction by depolarizing the membrane potential of vascular smooth muscle cells and subsequently activating L-type Ca^{2+} channels[48,49]. We found that the aorta from ND- and HFD + L-NAME-treated mice (28 weeks old) exhibited a loss of contractile response to PE, though they were still responsive to KPSS. However, the amplitude of KPSS-induced constriction of aorta from HFD + L-NAME-treated mice was lower than that from ND-treated mice. We thought that the loss of the contractile response to PE in aorta from HFD + L-NAME-treated mice was due to aging, because the contractile response to PE in aorta from the same-age ND group (28 weeks old) was similar. Since the contractile function of aorta in ND- and HFD + L-NAME-treated mice has altered, measurement of vasorelaxation would be inaccurate. Therefore, we compared the KPSS-induced constriction of aorta in mice of all groups. The KPSS-induced constriction of the mouse aorta from HFD + L-NAME group was decreased, and nitazoxanide and dapagliflozin treatments improved the impaired aorta constriction. Furthermore, tizoxanide directly relaxed PE- and U46619-induced vasoconstriction of rat mesenteric arteries. We thought that, on the one hand, tizoxanide showed vasorelaxant effects; on the other hand, tizoxanide improved aging-related pathology of arteries, both of these two aspects might contribute to the improvement of nitazoxanide on hypertension in the HFpEF model.

We thought that the effect of nitazoxanide on HFpEF and metabolic syndrome *in vivo* was global and systemic, we summarized the potential mechanisms of nitazoxanide against HFpEF and metabolic syndrome in Fig. 11. Apparently, in HFD + L-NAME "two-hit" model, multiple factors including endothelial injury, obesity, glucose and lipid metabolism disorders were implicated in the development of HFpEF, the *in vitro* experiments could not cover all the pathogenetic factors *in vivo*.

It was worth noting that a Phase 2a clinical trial was recently announced which evaluated the effects of HU6 on weight loss, body composition, exercise capacity, cardiac structure and function, metabolism, and inflammation in patients with obesity-related HFpEF[50]. HU6 is metabolized to 2,4-dinitrophenol *in vivo* to exert effects. 2,4-dinitrophenol is a classical mitochondrial uncoupler and had been used as a weight loss drug but unfortunately, it was withdrawn from the market for the significant adverse effects[51]. Now, it entered a Phase 2a clinical trial, suggesting that finding drugs based on the mitochondrial uncoupling mechanism is workable.

4.2. *Comparison with the HFpEF model previously reported*

In the present study, we used the same strain of C57BL/6N male mice as in previous works[13,21] to establish the HFpEF model. In the previous works[13,21], L-NAME was administered either through drinking water or embedded into the diet. To ensure the success of

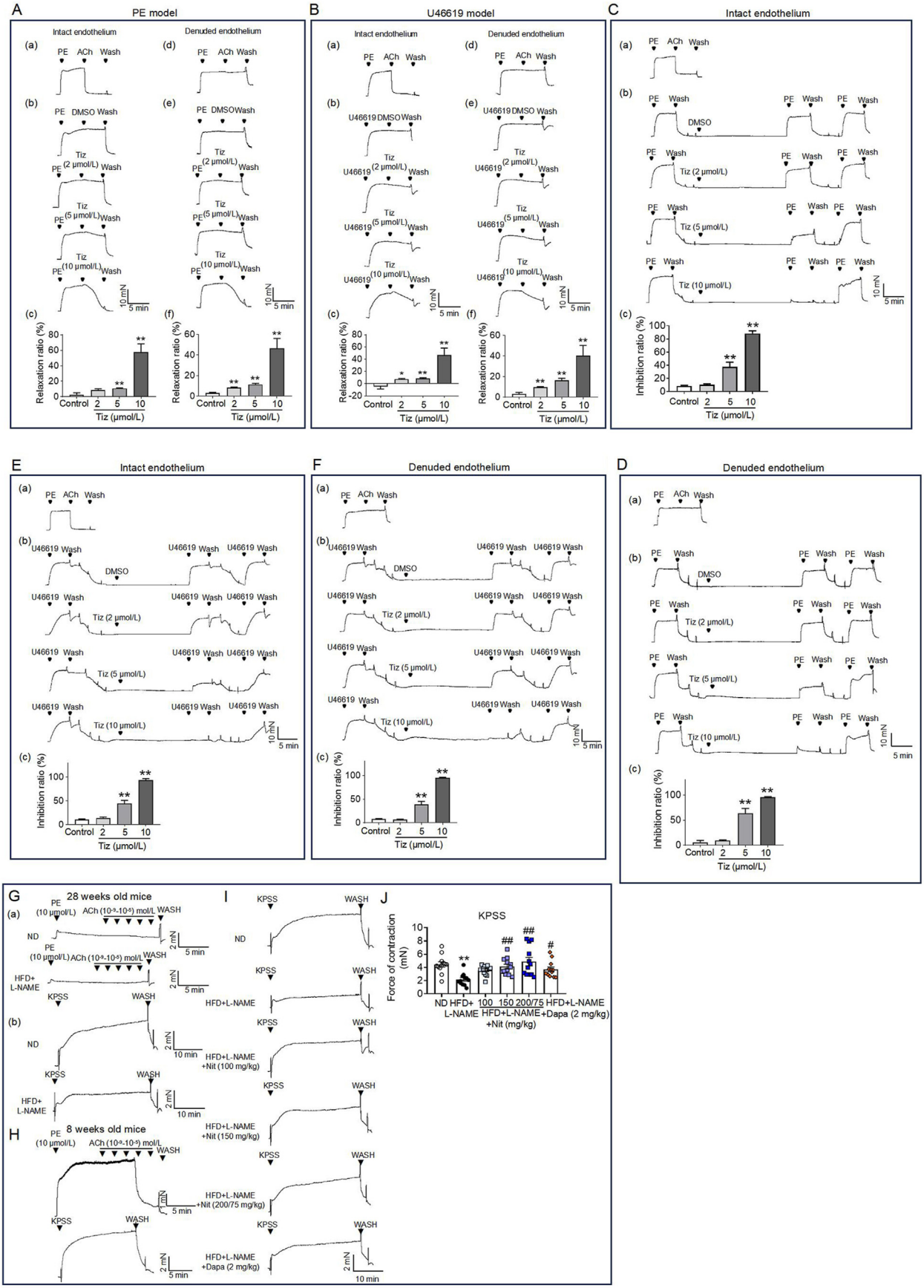
A
PE model
Intact endothelium
Denuded endothelium
B
U46619 model
C
Intact endothelium
D
Denuded endothelium
E
Intact endothelium
F
Denuded endothelium
PE
ACh
Wash
DMSO
Tiz (2 μmol/L)
Tiz (5 μmol/L)
Tiz (10 μmol/L)
U46619
Relaxation ratio (%)
Inhibition ratio (%)
Control
Tiz (μmol/L)
10 mN
5 min
G
28 weeks old mice
ND
HFD+ L-NAME
KPSS
WASH
2 mN
10 min
H
8 weeks old mice
I
HFD+L-NAME
HFD+L-NAME +Nit (100 mg/kg)
HFD+L-NAME +Nit (150 mg/kg)
HFD+L-NAME +Nit (200/75 mg/kg)
HFD+L-NAME +Dapa (2 mg/kg)
J
KPSS
Force of contraction (mN)
ND
HFD+ L-NAME
100
150
200/75
HFD+L-NAME +Nit (mg/kg)
HFD+L-NAME+Dapa (2 mg/kg)

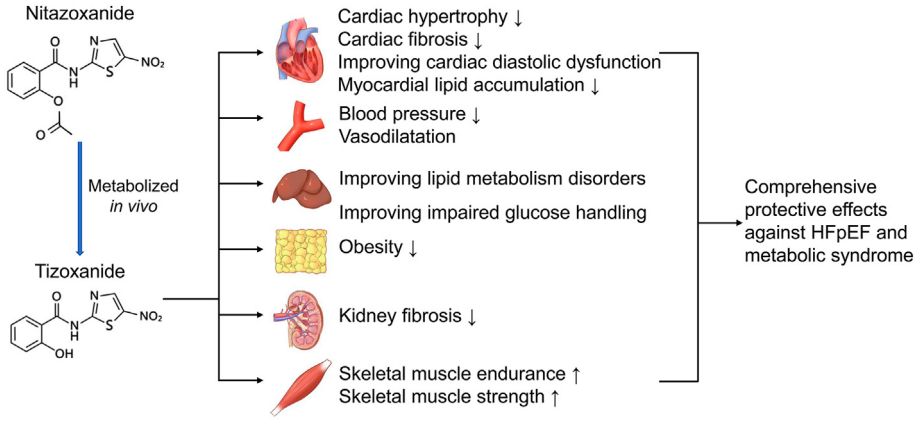

Figure 11 Schematic diagram of the potential mechanisms of nitazoxanide against HFpEF and metabolic syndrome.

model establishment, we embedded L-NAME in the HFD diet (1 g/kg) which was higher than that used (750 mg/kg) in the previous work[13]. The HFpEF phenotypes of mice in the present study were similar to those previously reported[13,21], including cardiac hypertrophy, cardiac diastolic dysfunction, increased blood pressure, impaired exercise tolerance, impaired glucose handling, etc. However, we did not detect the increase of lung weight or pathological changes in H&E-stained lung tissues in HFD + L-NAME treated mice, which was different from the previous works which showed the increased wet and dry lung weight in the HFD + L-NAME treated mice[21]. In the present study, we found that HFD + L-NAME treated mice exhibited typical hepatic steatosis, renal fibrosis and increased serum level of NT-proBNP, which were not documented in the previous works[13,21]. HFpEF generally coexists with hepatic steatosis, renal fibrosis and other metabolic disorders, and these disorders interact with each other to accelerate the progression of HFpEF[28,29,52]. Therefore, the present results further suggested the comprehensive mechanisms of nitazoxanide's effect.

4.3. Comparison of the effect of nitazoxanide and dapagliflozin on HFpEF and metabolic syndrome

In the present study, nitazoxanide was used *in vivo* at doses of 100, 150, 200/75 mg/kg, which covered the equivalent dose range in clinic. The aim of designing a dosage of 200/75 mg/kg has been explained in the Result-1 part. Comprehensively, the present results suggested that nitazoxanide at 150 mg/kg showed a relatively stronger effect than that at 100 and 200/75 mg/kg. However, all three dosages of nitazoxanide exhibited protective effects against HFpEF and metabolic syndrome induced by HFD + L-NAME in mice.

The present study showed that the effect of nitazoxanide and dapagliflozin on HFpEF and metabolic syndrome was similar as well as different. Both nitazoxanide and dapagliflozin treatments inhibited cardiac hypertrophy, cardiac fibrosis, improved cardiac diastolic dysfunction, and lowered blood pressure in the HFD + L-NAME-induced mouse model at a similar efficacy. However, nitazoxanide exhibited superior performance than dapagliflozin in improving metabolic syndrome. HFD + L-NAME induced typical hepatic steatosis, an increase of white adipose depots and serum lipids. Nitazoxanide treatment significantly improved the lipid deposition in livers, reduced liver TC and TG levels, decreased white adipose tissue weight, and ameliorated serum lipid disorders. Dapagliflozin showed a relatively weaker effect compared to nitazoxanide on the above-mentioned phenotypes.

HFpEF is classified into five subtypes, vascular-related HFpEF, cardiomyopathy-related HFpEF, right heart- and pulmonary-related HFpEF, valvular- and rhythm-related HFpEF, and extracardiac disease-related HFpEF[53]. The extracardiac diseases include diabetes mellitus, obesity, or metabolic syndrome. HFpEF patients may fall under one or more subtypes. According to the present results, we suggested that nitazoxanide was primarily recommended for extracardiac disease-related HFpEF therapy.

Dapagliflozin is a first-line drug for HFpEF therapy. Randomized clinical trials have demonstrated that it reduced heart failure hospitalization or cardiovascular death[54]. In the present study, we used dapagliflozin as a positive drug and the doses of both dapagliflozin and nitazoxanide were clinically equivalent.

Figure 10 Tizoxanide relaxes the constricted artery and pretreatment of tizoxanide inhibits artery constriction *ex vivo*. (A) Tizoxanide relaxed PE-induced vasoconstriction of rat mesenteric arteries with intact endothelium (a–c) and denuded endothelium (d–f). (B) Tizoxanide relaxed U46619-induced vasoconstriction of rat mesenteric arteries with intact endothelium (a–c) and denuded endothelium (d–f). (C) Tizoxanide pretreatment inhibited PE-induced vasoconstriction of rat mesenteric arteries with intact endothelium. (D) Tizoxanide pretreatment inhibited PE-induced vasoconstriction of rat mesenteric arteries with denuded endothelium. (E) Tizoxanide pretreatment inhibited U46619-induced vasoconstriction of rat mesenteric arteries with intact endothelium. (F) Tizoxanide pretreatment inhibited U46619-induced vasoconstriction of rat mesenteric arteries with denuded endothelium. Data are expressed as mean ± SEM, $n = 6–7$. $^{*}P < 0.05$, $^{**}P < 0.01$ *vs.* Control. (G) No contractile response of the aorta to PE (a) and KPSS (b) in mice from ND and HFD + L-NAME groups. The mice in the ND and HFD + L-NAME groups were 28 weeks old. (H) The contractile response of the aorta to PE and KPSS in mice (male 8-week-old C57BL/6N mice). (I, J) Nitazoxanide restored the decrease of KPSS-induced thoracic aorta contraction induced by HFD + L-NAME in mice. Data are expressed as mean ± SEM, $n = 12$. $^{**}P < 0.01$ *vs.* ND; $^{\#}P < 0.05$, $^{\#\#}P < 0.01$ *vs.* HFD + L-NAME. ACh, acetylcholine; Tiz, Tizoxanide; PE, phenylephrine; Nit, nitazoxanide; Dapa, dapagliflozin; KPSS, K^{+} physiological salt solution; HFD, high-fat diet; ND, normal diet.

The present results indicated that the comprehensive performance of nitazoxanide was superior to that of dapagliflozin.

5. Conclusions

Oral nitazoxanide at the clinically equivalent doses improved cardiac hypertrophy, cardiac fibrosis, cardiac diastolic dysfunction, increased blood pressure, impaired exercise tolerance, impaired glucose handling, serum lipid disorders, hepatic steatosis, increased weight of white adipose tissues and kidney fibrosis in HFD + L-NAME-induced HFpEF model in mice. We suggest that nitazoxanide is a potential drug for HFpEF and the related metabolic syndrome therapy.

Acknowledgments

This work was supported by the National Natural Science Foundation of China (Nos. 82373864 and 82170472).

Author contributions

Jiahui Chen: Investigation, Data curation. Liping Zhang: Investigation, Data curation. Ting Xie: Investigation, Data curation. Xiao Zhang: Investigation, Data curation. Congcong Pan: Investigation, Data curation. Fangli Sun: Investigation, Data curation. Wenfeng Li: Investigation, Data curation. Zhijie Sun: Writing − review & editing, Supervision, Project administration, Funding acquisition. Deli Dong: Writing − review & editing, Supervision, Project administration, Funding acquisition, Conceptualization.

Conflicts of interest

The authors declare that they have no competing interests.

Appendix A. Supporting information

Supporting information to this article can be found online at https://doi.org/10.1016/j.apsb.2024.12.040.

References

1. Kosiborod MN, Petrie MC, Borlaug BA, Butler J, Davies MJ, Hovingh GK, et al. Semaglutide in patients with obesity-related heart failure and type 2 diabetes. *N Engl J Med* 2024;**390**:1394−407.
2. Gao JL, Zhao J, Zhu HB, Peng X, Zhu JX, Ma MH, et al. Characterizations of mitochondrial uncoupling induced by chemical mitochondrial uncouplers in cardiomyocytes. *Free Radic Biol Med* 2018;**124**:288−98.
3. Zhang YQ, Shen X, Xiao XL, Liu MY, Li SL, Yan J, et al. Mitochondrial uncoupler carbonyl cyanide m-chlorophenylhydrazone induces vasorelaxation without involving K channel activation in smooth muscle cells of arteries. *Br J Pharmacol* 2016;**173**:3145−58.
4. Tai Y, Li LJ, Peng X, Zhu JX, Mao XH, Qin N, et al. Mitochondrial uncoupler BAM15 inhibits artery constriction and potently activates AMPK in vascular smooth muscle cells. *Acta Pharm Sin B* 2018;**8**:909−18.
5. Zhang XY, Zhang XZ, Zhang YQ, Liu MY, Jin J, Yan J, et al. Mitochondrial uncoupler triclosan induces vasorelaxation of rat arteries. *Acta Pharm Sin B* 2017;**7**:623−9.
6. Li SL, Yan J, Zhang YQ, Zhen CL, Liu MY, Jin J, et al. Niclosamide ethanolamine inhibits artery constriction. *Pharmacol Res* 2017;**115**:78−86.
7. Hu N, Fu Y, Li WF, Yang XR, Cao M, Li FF, et al. Chemical mitochondrial uncouplers share common inhibitory effect on NLRP3 inflammasome activation through inhibiting NFκB nuclear translocation. *Toxicol Appl Pharmacol* 2021;**414**:115426.
8. Ma MH, Li FF, Li WF, Zhao H, Jiang M, Yu YY, et al. Repurposing nitazoxanide as a novel anti-atherosclerotic drug based on mitochondrial uncoupling mechanisms. *Br J Pharmacol* 2023;**180**:62−79.
9. Rossignol JF, Elfert A, El Gohary Y, Keeffe EB. Improved virologic response in chronic hepatitis C genotype 4 treated with nitazoxanide, peginterferon, and ribavirin. *Gastroenterology* 2009;**136**:856−62.
10. Rossignol JF, Bréchot C. A pilot clinical trial of nitazoxanide in the treatment of chronic hepatitis B. *Hepatol Commun* 2019;**3**:744−7.
11. Li FF, Jiang M, Ma MH, Chen XY, Zhang YD, Zhang YX, et al. Anthelmintics nitazoxanide protects against experimental hyperlipidemia and hepatic steatosis in hamsters and mice. *Acta Pharm Sin B* 2022;**12**:1322−38.
12. Li WF, Chen SM, Lang J, Luo J, Chen JH, Zhang LP, et al. The clinical antiprotozoal drug nitazoxanide and its metabolite tizoxanide extend *Caenorhabditis elegans* lifespan and healthspan. *Acta Pharm Sin B* 2024;**14**:3266−80.
13. Schiattarella G, Altamirano F, Kim S, Tong D, Ferdous A, Piristine H, et al. Xbp1s−FoxO1 axis governs lipid accumulation and contractile performance in heart failure with preserved ejection fraction. *Nat Commun* 2021;**12**:1684.
14. Chen XY, Dong YC, Yu YY, Jiang M, Bu WJ, Li P, et al. Anthelmintic nitazoxanide protects against experimental pulmonary fibrosis. *Br J Pharmacol* 2023;**180**:3008−23.
15. Jiang M, Zhang YX, Bu WJ, Li P, Chen JH, Cao M, et al. Piezo1 channel activation stimulates ATP production through enhancing mitochondrial respiration and glycolysis in vascular endothelial cells. *Br J Pharmacol* 2023;**180**:1862−77.
16. Liu MY, Jin J, Li SL, Yan J, Zhen CL, Gao JL, et al. Mitochondrial fission of smooth muscle cells is involved in artery constriction. *Hypertension* 2016;**68**:1245−54.
17. Zhao J, Gao JL, Zhu JX, Zhu HB, Peng X, Jiang M, et al. The different response of cardiomyocytes and cardiac fibroblasts to mitochondria inhibition and the underlying role of STAT3. *Basic Res Cardiol* 2019;**114**:12.
18. Fu Y, Hu N, Cao M, Li WF, Yang XR, Gao JL, et al. Anthelmintic niclosamide attenuates pressure-overload induced heart failure in mice. *Eur J Pharmacol* 2021;**912**:174614.
19. Ibrahim A, Yucel N, Kim B, Arany Z. Local mitochondrial ATP production regulates endothelial fatty acid uptake and transport. *Cell Metab* 2020;**32**:309−19.e7.
20. Curtis MJ, Alexander S, Cirino G, Docherty JR, George CH, Giembycz MA, et al. Experimental design and analysis and their reporting II: updated and simplified guidance for authors and peer reviewers. *Br J Pharmacol* 2018;**175**:987−93.
21. Schiattarella GG, Altamirano F, Tong D, French KM, Villalobos E, Kim SY, et al. Nitrosative stress drives heart failure with preserved ejection fraction. *Nature* 2019;**568**:351−6.
22. Solomon SD, McMurray JJV, Claggett B, de Boer RA, DeMets D, Hernandez AF, et al. Dapagliflozin in heart failure with mildly reduced or preserved ejection fraction. *N Engl J Med* 2022;**387**:1089−98.
23. Nassif ME, Windsor SL, Borlaug BA, Kitzman DW, Shah SJ, Tang F, et al. The SGLT2 inhibitor dapagliflozin in heart failure with preserved ejection fraction: a multicenter randomized trial. *Nat Med* 2021;**27**:1954−60.
24. Ponikowski P, Voors AA, Anker SD, Bueno H, Cleland JG, Coats AJ, et al. 2016 ESC guidelines for the diagnosis and treatment of acute and chronic heart failure: the task force for the diagnosis and treatment of acute and chronic heart failure of the European Society of Cardiology (ESC). developed with the special contribution of the Heart Failure Association (HFA) of the ESC. *Eur J Heart Fail* 2016;**18**:891−975.
25. Nasiri Ansari N, Androutsakos T, Flessa CM, Kyrou I, Siasos G, Randeva HS, et al. Endothelial cell dysfunction and nonalcoholic fatty liver disease (NAFLD): a concise review. *Cells* 2022;**11**:2511.
26. Steinberg GR, Hardie DG. New insights into activation and function of the AMPK. *Nat Rev Mol Cell Biol* 2023;**24**:255−72.

27. Jin X, Qiu T, Li L, Yu R, Chen X, Li C, et al. Pathophysiology of obesity and its associated diseases. *Acta Pharm Sin B* 2023;**13**:2403−24.
28. Valero Muñoz M, Oh A, Faudoa E, Bretón Romero R, El Adili F, Bujor A, et al. Endothelial−mesenchymal transition in heart failure with a preserved ejection fraction: insights into the cardiorenal syndrome. *Circ Heart Fail* 2021;**14**:e008372.
29. Ter Maaten JM, Damman K, Verhaar MC, Paulus WJ, Duncker DJ, Cheng C, et al. Connecting heart failure with preserved ejection fraction and renal dysfunction: the role of endothelial dysfunction and inflammation. *Eur J Heart Fail* 2016;**18**:588−98.
30. Liu KX, Wang ZY, Ying YT, Wei RM, Dong DL, Sun ZJ. The antiprotozoal drug nitazoxanide improves experimental liver fibrosis in mice. *Biochem Pharmacol* 2024;**224**:116205.
31. Leggat J, Bidault G, Vidal Puig A. Lipotoxicity: a driver of heart failure with preserved ejection fraction?. *Clin Sci (Lond)* 2021;**135**:2265−83.
32. Nowinski SM, Solmonson A, Rundhaug JE, Rho O, Cho J, Lago CU, et al. Mitochondrial uncoupling links lipid catabolism to Akt inhibition and resistance to tumorigenesis. *Nat Commun* 2015;**6**:8137.
33. Gélinas R, Mailleux F, Dontaine J, Bultot L, Demeulder B, Ginion A, et al. AMPK activation counteracts cardiac hypertrophy by reducing *O*-GlcNAcylation. *Nat Commun* 2018;**9**:374.
34. Zhuang LF, Jia KN, Chen C, Li ZG, Zhao JX, Hu J, et al. DYRK1B−STAT3 drives cardiac hypertrophy and heart failure by impairing mitochondrial bioenergetics. *Circulation* 2022;**145**:829−46.
35. Chaanine AH, Hajjar RJ. AKT signalling in the failing heart. *Eur J Heart Fail* 2011;**13**:825−9.
36. Chan AY, Dolinsky VW, Soltys CL, Viollet B, Baksh S, Light PE, et al. Resveratrol inhibits cardiac hypertrophy *via* AMP-activated protein kinase and Akt. *J Biol Chem* 2008;**283**:24194−201.
37. Li Y, Zhang H, Liao WQ, Song Y, Ma XW, Chen C, et al. Transactivated EGFR mediates α_1-AR-induced STAT3 activation and cardiac hypertrophy. *Am J Physiol Heart Circ Physiol* 2011;**301**:H1941−51.
38. Meijles DN, Fuller SJ, Cull JJ, Alharbi HO, Cooper STE, Sugden PH, et al. The insulin receptor family and protein kinase B (Akt) are activated in the heart by alkaline pH and α_1-adrenergic receptors. *Biochem J* 2021;**478**:2059−79.
39. Jiang H, Yang JJ, Li T, Wang XY, Fan ZC, Ye Q, et al. JAK/STAT3 signaling in cardiac fibrosis: a promising therapeutic target. *Front Pharmacol* 2024;**15**:1336102.
40. Withaar C, Lam CSP, Schiattarella GG, de Boer RA, Meems LMG. Heart failure with preserved ejection fraction in humans and mice: embracing clinical complexity in mouse models. *Eur Heart J* 2021;**42**:4420−30.
41. Elaidy SM, Hussain MA, El Kherbetawy MK. Time-dependent therapeutic roles of nitazoxanide on high-fat diet/streptozotocin-induced diabetes in rats: effects on hepatic peroxisome proliferator-activated receptor-gamma receptors. *Can J Physiol Pharmacol* 2018;**96**:485−97.
42. Anderson VR, Curran MP. Nitazoxanide: a review of its use in the treatment of gastrointestinal infections. *Drugs* 2007;**67**:1947−67.
43. Caldeira da Silva CC, Cerqueira FM, Barbosa LF, Medeiros MHG, Kowaltowski AJ. Mild mitochondrial uncoupling in mice affects energy metabolism, redox balance and longevity. *Aging Cell* 2008;**7**:552−60.
44. Childress ES, Alexopoulos SJ, Hoehn KL, Santos WL. Small molecule mitochondrial uncouplers and their therapeutic potential. *J Med Chem* 2018;**61**:4641−55.
45. Goedeke L, Shulman GI. Therapeutic potential of mitochondrial uncouplers for the treatment of metabolic associated fatty liver disease and NASH. *Mol Metab* 2021;**46**:101178.
46. Seals D, Jablonski K, Donato A. Aging and vascular endothelial function in humans. *Clin Sci* 2011;**120**:357−75.
47. Deckert V, Lizard G, Duverger N, Athias A, Palleau V, Emmanuel F, et al. Impairment of endothelium-dependent arterial relaxation by high-fat feeding in ApoE-deficient mice: toward normalization by human ApoA-I expression. *Circulation* 1999;**100**:1230−5.
48. Jin J, Shen X, Tai Y, Li SL, Liu MY, Zhen CL, et al. Arterial relaxation is coupled to inhibition of mitochondrial fission in arterial smooth muscle cells: comparison of vasorelaxant effects of verapamil and phentolamine. *Acta Pharm Sin B* 2017;**7**:319−25.
49. Küng CF, Moreau P, Takase H, Lüscher TF. L-NAME hypertension alters endothelial and smooth muscle function in rat aorta. Prevention by trandolapril and verapamil. *Hypertension* 1995;**26**:744−51.
50. Kitzman DW, Lewis GD, Pandey A, Borlaug BA, Sauer AJ, Litwin SE, et al. A novel controlled metabolic accelerator for the treatment of obesity-related heart failure with preserved ejection fraction: rationale and design of the phase 2a HuMAIN trial. *Eur J Heart Fail* 2024;**26**:2013−24.
51. Grundlingh J, Dargan PI, El Zanfaly M, Wood DM. 2,4-Dinitrophenol (DNP): a weight loss agent with significant acute toxicity and risk of death. *J Med Toxicol* 2011;**7**:205−12.
52. Salah HM, Pandey A, Soloveva A, Abdelmalek MF, Diehl AM, Moylan CA, et al. Relationship of nonalcoholic fatty liver disease and heart failure with preserved ejection fraction. *JACC Basic Transl Sci* 2021;**6**:918−32.
53. Ge J. Coding proposal on phenotyping heart failure with preserved ejection fraction: a practical tool for facilitating etiology-oriented therapy. *Cardiol J* 2020;**27**:97−8.
54. Redfield MM, Borlaug BA. Heart failure with preserved ejection fraction: a review. *JAMA* 2023;**329**:827−38.